Auburn University

B-425

Report of Statnanic Tests on Rock Sockets at Spring Villa, Alabama

Prepared by

Dan A. Brown, Gottlieb Associate Professor of Civil Engineering

Highway Research Center
Harbert Engineering Center
Auburn University, Alabama 36849-5337

November 2002

REPORT OF STATNAMIC TESTS ON ROCK SOCKETS AT SPRING VILLA, ALABAMA

INTRODUCTION

This test program consists of a series of lateral load tests performed on rock sockets at Auburn University test site located in Spring Villa, Alabama, including static tests, direct shear tests, lateral Osterberg tests and Statnamic load tests. This report mainly presents the results from Statnamic load tests. Results from other tests have been reported by Kahle (2000). The objectives of this test program are to produce additional data for full-scale load tests in weathered rock, to determine the strength of the rock and to verify the available design methods. The test site is part of Southern Piedmont area, and rocks were composed of sedimentary deposits of sand, mud and carbonate along an ancient ocean that were transformed into metamorphic quartzite, schist and marble.

A total of four Statnamic tests were performed on rock sockets with diameter ranging from 3ft to 5ft and depth ranging from 3ft to 7.5ft. A brief site plan is shown in Figure 1, along with other test shafts on which the static tests were conducted. 17 shafts were constructed with a diameter of 5ft and 3ft. For shafts with 5ft diameter, the shaft extended to 5ft or 7.5ft below the ground level. For shafts with 3ft diameter, the shafts extended to 3ft or 6ft below the ground level. As indicated in Figure 1, Statnamic test was conducted on shaft A2, A3, B5 and B6 respectively. Static test was performed on other shafts. Each test shaft was instrumented with load cell, displacement transducers and accelerometers to measure the load, displacement and acceleration response. All the sensors were wired into Megadac data collector and then connected to a computer.

SITE CHARACTERIZATION

As mentioned above, the test site mainly consists of heavily weathered rock. The Alabama Department of Transportation (ALDOT) has performed eight borings on the test site till a depth of 30ft. It was concluded that there is approximately 4 to 8 feet hard tan-brown silt overlying a 1 to 2.5 feet layer of very weathered, soft to medium rock on the far eastern side of the test area. And the soft rock is underlain by hard fractured quartzite. The borings from the western side of the test area indicated a 3.5ft tan-brown silt layer overlying 2' thick weathered soft rock that is underlain by hard layers.

SPT test was also performed every 1.5ft until the underlying rock was reached by the auger. The SPT-N value was in a range of 26 to 63 blows/ft in the upper layers of brown silt and increased to over 100 blows/ft as the auger reached rock. In order to obtain the strength parameters of quartzite, rock cores were tested, indicating only 2-18% core recovery and 0% rock quality designation (RQD). However, the rock cores could not be used in the unconfined compression test, so no strength property was determined.

STATNAMIC LOAD TEST

The Statnamic load test provides a method for generating large axial or lateral loads on foundations by launching a heavy reaction mass away from the foundation at an acceleration approaching 20 g's. The energy for the test is generated by burning special fuel pellets in a combustion chamber inside the Statnamic device, and allowing the resulting high pressure gas to vent at a controlled rate, which in turn controls the rate at which the foundation is loaded. The reaction mass is initially set up against the side of the foundation and imparts a load that ramps up to its maximum value in a finite amount of

time, usually between 0.1 and 0.3 seconds, and then gradually decreases as the mass is propelled away from the foundation and physical contact between the foundation and the reaction mass ceases. The load is not a sharp impact, but is similar to the case where a moving barge might impact a bridge foundation, even though the ramp time for the latter case may be several times larger depending on the mass of the barge and the speed at which it was moving. The primary advantages of the Statnamic test are that it is quick, it provides energy in a frequency band close to the fundamental frequency of the foundation, and it produces significant inertial forces in the system, which allows the determination of dynamic system properties. The Statnamic testing system is manufactured by Berminghammer Foundation Equipment of Hamilton, Ontario.

TEST SETUP

As shown in Figure 1, Statnamic tests were performed on four shafts, which are shaft A2, A3, B5 and B6, each with 3 or 4 shots. Each test recorded a total of 13 channels of data sampled at 2000Hz. During each test, the test shaft was fully instrumented to measure the displacement, acceleration and load time history. The following is the instrumentation used in the test:

1 Load Cell,

2 Displacement Transducers (LVDTs),

10 Accelerometers.

The detailed instrumentation for each test shaft is shown in Figure 2 to Figure 5. The two LVDTs were mounted to the backside of the shaft at the elevation close to the load applied so as to get the approximate displacement at the load point. The ten

accelerometers were placed in multiple configurations. Four of them were oriented at about the same location as the two LVDTs to measure the axial and lateral acceleration. This provided a way to check the LVDT results by integrating the lateral acceleration response twice. Another one was placed to the front side of the shaft measuring axial acceleration. Five additional accelerometers were mounted to five small probes and slid down the inclinometer casing cast in the test shaft. These five accelerometers were arranged in a chain spaced at 18" to measure the lateral acceleration at different depths. The lateral displacement along the length of the shaft can be obtained using these downhole accelerometers' signals.

The load cell, LVDTs and accelerometers were wired to the Megadac data acquisition system to record the signal at a rate of 2000Hz. The Megadac system was controlled by a laptop computer using the Test Control Software (TCS) and an IEEE-488 data interface. Test data saved by TCS were exported to various formats like ASCII and Matlab for further analysis.

LOAD AND DISPLACEMENT TIME HISTORY

For test shaft A2, three tests were performed with a peak load of 408KN, 954KN and 1544KN. Figure 6 presents the load time histories for all three shots. The loading impulse ranged between about 0.15s to 1.0s, with the larger load ramping up faster. The maximum load of each shot for all test shafts was summarized in Table 1, along with the corresponding mobilized displacement. The load time histories of test shaft A3, B5 and B6 are shown in Figure 7 to Figure 9 respectively. Each test shaft was loaded four times. Note for shaft B6, the load pulse has unusual shape. For test 2 as shown in Figure 6, the

recording time seems delayed, but the peak load ramped up faster than test 1 and slower than test 3 as other test shafts. For shaft A3, the peak load for 4 load cases was 417KN, 986KN, 1498KN and 1879KN respectively. While for shaft B5 and B5 with smaller diameter, the applied load was much less than shaft A2 and A3. For shaft B5 with a larger depth, the maximum load in load case 4 was 870KN. The maximum load for shaft B6 was only 581KN; this is because the depth of shaft B5 is only 3ft and there is no enough soil resistance to carry large load.

Lateral displacement was monitored using two displacement transducers along the test shaft. The lateral displacement of shafts was represented by the displacement at the load elevation, which can be calculated by interpolating (or extrapolating) the results of top LVDT and bottom LVDT. This lateral displacement response for each load case of every test shaft is shown in Figure 10 to Figure 13 respectively. For each case, the lateral displacement ramps up to a peak value; then oscillates several times before damping out. The oscillation damps out quickly at lower applied loads, but increases with the increase of the applied loads. For shaft A2, the peak lateral displacement of three cases is 1.9mm, 9.9mm and 25.5mm respectively. A summary of peak displacement for each case is shown in Table 1. Comparison of load and displacement time history shows that the displacement response is a little delayed. The maximum displacement is reached slightly later than the peak load.

EQUIVALENT SINGLE DEGREE OF FREEDOM SYSTEM MODEL

The dynamic response of each test shaft has been modeled using an equivalent single-degree-of-freedom (SDOF) system. The dynamic response of an SDOF system is governed by the following differential equation:

$$Mu'' + Cu' + Ku = F(t) \quad (1)$$

where u'', u', and u represent the acceleration, velocity and displacement of the system, respectively, that define the physical state of the system at any instant of time, t. $F(t)$ represents the forcing function vector. M, C and K are the generalized mass, damping and stiffness coefficients of the SDOF system that may or may not change over time, with frequency of motion or with amplitude of motion. The mass and the damping coefficient were considered constant during a single loading event. For all four test shafts, the load-displacement response was highly nonlinear, so it is very difficult to model the stiffness coefficient K as a function of displacement, u. In the analysis, K was assumed unchanged in each load case and changing from one load case to another.

Equation (1) may also be expressed as follows:

$$F_{inertia} + F_{damping} + F_{static} = F_{statnamic} \quad (2)$$

where

$F_{inertia}$ = inertial resistance from effective mass of the foundation,

$F_{damping}$ = effective viscous damping resistance,

F_{static} = effective static soil resistance, and

$F_{statnamic}$ = measured force on the Statnamic load cell.

The Newmark-β integration algorithm was used to solve the dynamic equation of motion numerically. Assuming the acceleration varied linearly between consecutive time steps, the response at any time could be computed using a total force balance and the state of the system at the previous step. The solution was implemented using a Matlab program with a graphic user interface whose input consisted of the measured Statnamic load vector $F(t)$ and the values of the system parameters M, C and K. The response of the system was obtained by interactively changing the values of M, C and K until a good match was noted between the measured displacement time history (signals from the displacement transducers), and the simulated response (computed for the SDOF model). The goodness of match between the model response and the measured response was judged by eye by plotting the time histories simultaneously on the same graph. In most cases it was possible to arrive at a good match between the measured and computed time histories with a relatively small number of trials. The procedure used for signal matching can be broadly divided into the following steps:

1. Determine the mass coefficient by computing the mass of the foundation above the ground line. The actual participating mass may vary slightly from this number, and M may be changed slightly (± 5 %, but usually slightly more) during the trials to establish a better match.
2. Estimate the lateral static stiffness of the foundation and use this value as a starting point for the stiffness parameter K. Compare the first peak in the computed displacement response with the first peak in the measured response and determine if K appears reasonable. Increase or decrease K until a good match is achieved for the amplitude of the first peak. It may

also be necessary to vary the mass parameter M slightly to match the phase of the simulated response to the measured response where the displacement ramps up to its first peak. If M is chosen too large, the computed displacement response will lag the measured response.

3. Finally, adjust the value of the damping coefficient by changing the damping ratio until the post loading free vibration parts of the measured and computed displacement response are in good agreement. The measured response may be affected by significant permanent deformations, but this cannot be simulated using the simplified SDOF model. The objective, however, is to estimate the amount of damping present in the system, and this can be done by comparing the amplitude decay pattern and the damped frequency of free vibration.

The numerical value of the viscous damping constant ("dashpot"), C, has relatively little effect on the response magnitude during the actual loading event, but is significant in determining the amplitude of decay and the damped free vibration frequency for post-loading response. In order to relate C more meaningfully to a system damping parameter, the damping constant may also be expressed as a percent of the critical damping constant C_c as follows:

$$\xi = C/C_c = C/[2(KM)^{1/2}] \tag{3}$$

where ξ is termed the "damping ratio" and

$$F_{damping} = 2\,\xi\,(KM)^{1/2}\,u' \tag{4}$$

The magnitude of the first peak in the simulated displacement time history is sensitive to the value of the effective stiffness parameter chosen, K. The stiffness term

also effects the frequency of damped free vibration at the end of the Statnamic loading event. K is also used to back calculate a derived static load-displacement response, which may be compared to the load-displacement function obtained from a conventional static test.

SDOF Model of Shaft A2

Each load case was simulated individually, with stiffness K changing from one load case to another and remain the constant during the same load case. The damping ratio was assumed to be constant through all three tests. The model parameters were adjusted by trial and error until a good match was obtained between the measured and computed response.

Figure 14 shows the measured and computed displacement response for all three tests of shaft A2, and also the derived displacement response from the accelerometers for load case 3. For the first 2 tests, the displacement was relatively small and the accelerometers signal was influenced a lot by noise, so integrating the signal could not give the accurate displacement results. The SDOF model results match the measured displacement quite well, with the measurement showing more residual displacement. However, this difference becomes smaller with the increase of the applied load because the residual displacement is insignificant relative to the peak displacement. The parameters used in the analysis are shown as below:

Mass: 20000Kg,

Damping Ratio: 0.60,

Stiffness Degradation Factor: 1.0,

Stiffness for Load Case 1: 220MN/m,

Stiffness for Load Case 2: 95MN/m,

Stiffness for Load Case 3: 56MN/m.

Note the mass was estimated by calculating the self weight of the test shaft. A summary of the SDOF model results for shaft A2 is shown in Table 2. *Fs* denotes the peak equivalent static force and is calculated as the product of the stiffness and the peak computed displacement. The total derived soil resistance is calculated as the sum of the equivalent static force and the damping force, and the damping force is computed as the product of the damping coefficient and the velocity. So it is a function of the time rate at which the shaft is loaded. *Fd* is the peak derived soil resistance and *Ud* is the displacement at which *Fd* occurs. Note that *Fd* is not the sum of *Fs* and the maximum damping force because the static force and the damping force do not necessarily reach the maximum value simultaneously.

Figure 15 is a plot of the derived load versus displacement response from the Statnamic tests for shaft A2. The load-displacement relationship exhibits nonlinear behavior, with the stiffness decreasing with the increasing of the displacement. The peak static force lags the peak total soil resistance for all load cases, with the phase difference increasing with increasing the applied loads and damping forces in the system. As shown in Figure 15, shaft A2 has high stiffness and didn't reach the yield point after 3 load cases.

SDOF Model of Shaft A3

The SDOF model of shaft A3 was obtained using the similar analysis as shaft A2. The lateral displacement response was computed using different input parameters until a good match between computed and measured displacement response was reached. Figure 16 shows the comparison between the measured and computed displacement response, also the derived displacement from the measured acceleration as mentioned before. The three set of results match well especially the first peak of the displacement response. The following is a list of modeling parameters used in the analysis.

Mass:	20000Kg
Damping Ratio:	0.60
Stiffness Degradation Factor:	1.0
Stiffness for Load Case 1:	99MN/m,
Stiffness for Load Case 2:	45MN/m,
Stiffness for Load Case 3:	21MN/m,
Stiffness for Load Case 4:	8.5MN/m.

The modeling results are summarized in Table 3. Note for load case 4, both static and dynamic force are less than case 3, indicating the yield of the system. The data in Table 3 were also plotted in Figure 17, including both equivalent static and total soil resistance as a function of the peak displacement. For first load case, the derived static and total force are very close, showing little damping force. But with the increasing of the applied load, the damping force becomes larger and the static peak force begins to lag the peak total soil resistance by a large amount at higher applied load. The displacement response is highly nonlinear, and the shaft began to fail in load case 4.

SDOF Model of Shaft B5

As before, shaft B5 was modeled using the following parameters. The mass of shaft B5 is smaller than shaft A2 and A3.

Mass:	14000Kg
Damping Ratio:	0.60
Stiffness Degradation Factor:	1.0
Stiffness for Load Case 1:	42MN/m
Stiffness for Load Case 2:	34MN/m
Stiffness for Load Case 3:	16MN/m
Stiffness for Load Case 4:	8.0MN/m.

Figure 18 presents the comparison of the measured lateral displacement and computed lateral displacement for all four load cases, and also the results obtained from the measurements of accelerometers. Three sets of curves match well, especially the first peak of the displacement response. But the results derived from accelerometers' measurement seem to oscillate before the maximum displacement occurs. Compared to calculated results, the LVDT measurements show a larger residual displacement as before.

The SDOF model results for shaft B5 are summarized Table 4 and also presented in Figure 19. Similar to shaft A3, the shaft began to fail in load case 4. However, for the total soil resistance (static force plus damping force), no failure was observed. For the first load case, the derived static and total force are almost equal and the displacement at which the maximum value occurs is the same. But with the increase of the applied load, the damping force increases and the difference of displacement becomes larger.

SDOF Model of Shaft B6

The SDOF model analysis for shaft B6 is similar to that of shaft A2, A3 and B5, with the following parameters. The mass is same as shaft B5. Different from other test shafts, the stiffness of load case 2 is even larger than load case 1.

Mass:	14000Kg
Damping Ratio:	0.60
Stiffness Degradation Factor:	1.0
Stiffness for Load Case 1:	13MN/m
Stiffness for Load Case 2:	14.5MN/m
Stiffness for Load Case 3:	9.0MN/m
Stiffness for Load Case 4:	2.8MN/m.

The comparison of displacement time history obtained from LVDT measurement, SDOF model and accelerometers' measurement is shown in Figure 20. For load case 1 and 2, the acceleration is relatively small and was influenced by noise, so the displacement derived from accelerometers' readings is not reliable. For the other two load cases, the three curves match fairly well, but there is some difference after the maximum displacement is reached.

Table 5 summarizes the SDOF modeling results of shaft B6. The data in Table 5 was also plotted in Figure 21. Similarly, with the increase of the applied load, the stiffness of the shaft decrease, and the phase difference between the derived static and total force increases. Also, the difference between the derived static and total force becomes larger, indicating greater damping force.

Comparison with Similar Static Tests

As mentioned before, a series of static tests were performed on the similar shafts at the same test site. Displacement transducers and load cell were installed to record the load and displacement response. The static load versus displacement curves can be obtained and compared with SDOF model results from the Statnamic tests discussed above. Figure 22 to Figure 25 present the comparison of load versus displacement derived from the Statnamic tests and the equivalent static tests.

For shaft A2, the derived load-displacement curve was compared with static test results of shaft C2 and F2, as shown in Figure 22. The measured static response is slightly stiffer than the derived static response at small displacement. But the derived static curve gives a higher capacity because shaft A2 did not fail at last data point while shaft F2 yielded at similar load level. Same trend can also be found from Figure 23 to Figure 25.

DISPLACEMENT PROFILE ALONG PILE LENGTH

Each shaft was instrumented with five downhole accelerometers at different depths along the shaft length, so a deflection versus depth curve can be obtained by integrating the acceleration information using the same technique as before. However, for some load cases where the induced acceleration (displacement) is small, it is difficult to get the correct displacement response from acceleration data because noise had a significant influence on accelerometers' signals. For large applied load, the displacement response derived from the acceleration is quite accurate, which can be seen from the comparison with the LVDT measurement.

For test shaft A2, deflection-depth curve (shown in Figure 26) was obtained only from load case 3, where the induced displacement is large enough that the influence of noise is insignificant. The deflection versus depth is almost a straight line from the top of the shaft to the ground surface because no resistance exists. Below the ground surface, the deflection decreases to a negative value close to the base of the shaft. The deflection curve for test shaft A3, B5 and B6 for three load cases are presented in Figure 27 to Figure 29 respectively. The results for shaft A3, B5 and B6 are consistent with shaft A2. The deflection close to the shaft base is negative and this value increases with the increasing of the applied load.

SUMMARY

This report presents the Statnamic testing results on four rock sockets embedded in heavily weathered rock. The dimensions of the test shaft were 5' diameter by 7.5ft deep, 5' diameter by 5ft deep, 3' diameter by 6ft deep and 3' diameter by 3ft deep respectively. Each test shaft was instrumented with load cell, LVDTs and accelerometers to monitor the response. The testing results can be summarized as follows:

1. The Statnamic loading impulse ranges from 0.15 to 1.0 seconds, with the larger load ramping up faster. The displacement response slightly lags the loading impulse.
2. The accelerometer measurements verify the LVDT measurement. The displacement response derived from accelerometers' signal is consistent with LVDT results.

3. The SDOF model appears to provide a relatively good way to interpret Statnamic testing results. The derived displacement response matches LVDT measurements fairly well. Using this model, the equivalent static load-displacement curve can be obtained. Comparison with the similar static test results indicates that the Statnamic tests show larger capacities than the static tests, but the shaft behavior is a little weaker than the static tests at small displacement.
4. The downhole accelerometer measurements provide a way to estimate the deflection profile along the shaft length. The deflection-depth curve is approximately a straight line above the ground level.

REFERENCES:

Kahle K.J. (2000). "Performance of Laterally Loaded Drilled Sockets Founded in Weathered Quartzite", December 16, 2000.

Table 1 Summary of Maximum Load and Displacement

Test Shaft		Maximum Load (KN)	Maximum Displacement (mm)
Shaft A2	Load Case 1	408.1	1.9
	Load Case 2	954.0	9.9
	Load Case 3	1544.0	25.5
Shaft A3	Load Case 1	417.3	4.6
	Load Case 2	986.0	20.6
	Load Case 3	1498.5	55.0
	Load Case 4	1870.5	106.5
Shaft B5	Load Case 1	176.9	4.2
	Load Case 2	414.1	12.0
	Load Case 3	708.7	40.4
	Load Case 4	869.8	79.8
Shaft B6	Load Case 1	130.5	10.1
	Load Case 2	230.1	15.8
	Load Case 3	354.9	37.2
	Load Case 4	581.3	125.3

Table 2 Summary of SDOF Model Results, Test Shaft A2

SDOF Model Results for Shaft A2				
Load Case	*Us* (mm)	*Fs* (KN)	*Ud* (mm)	*Fd* (KN)
1	1.9	408.3	1.8	413.0
2	10.0	951.1	9.4	1033.0
3	25.9	1452.1	22.5	1719.5

Table 3 Summary of SDOF Model Results, Shaft A3

SDOF Model Results for Shaft A3				
Load Case	*Us* (mm)	*Fs* (KN)	*Ud* (mm)	*Fd* (KN)
1	4.6	418.9	4.4	432.6
2	21.1	947.7	19.3	1088.4
3	54.9	1153.0	45.5	1580.4
4	106.9	908.9	77.9	1506.2

Table 4 Summary of SDOF Model Results, Shaft B5

SDOF Model Results for Shaft B5				
Load Case	*Us* (mm)	*Fs* (KN)	*Ud* (mm)	*Fd* (KN)
1	4.2	177.2	4.2	179.5
2	12.2	414.6	11.8	435.5
3	40.5	648.1	37.3	779.9
4	78.2	625.7	65.9	881.0

Table 5 Summary of SDOF Model Results, Shaft B6

SDOF Model Results for Shaft B6				
Load Case	*Us* (mm)	*Fs* (KN)	*Ud* (mm)	*Fd* (KN)
1	10.0	130.3	9.9	132.8
2	15.5	229.9	15.2	241.8
3	36.6	329.3	33.9	384.4
4	124.9	349.9	100.4	538.2

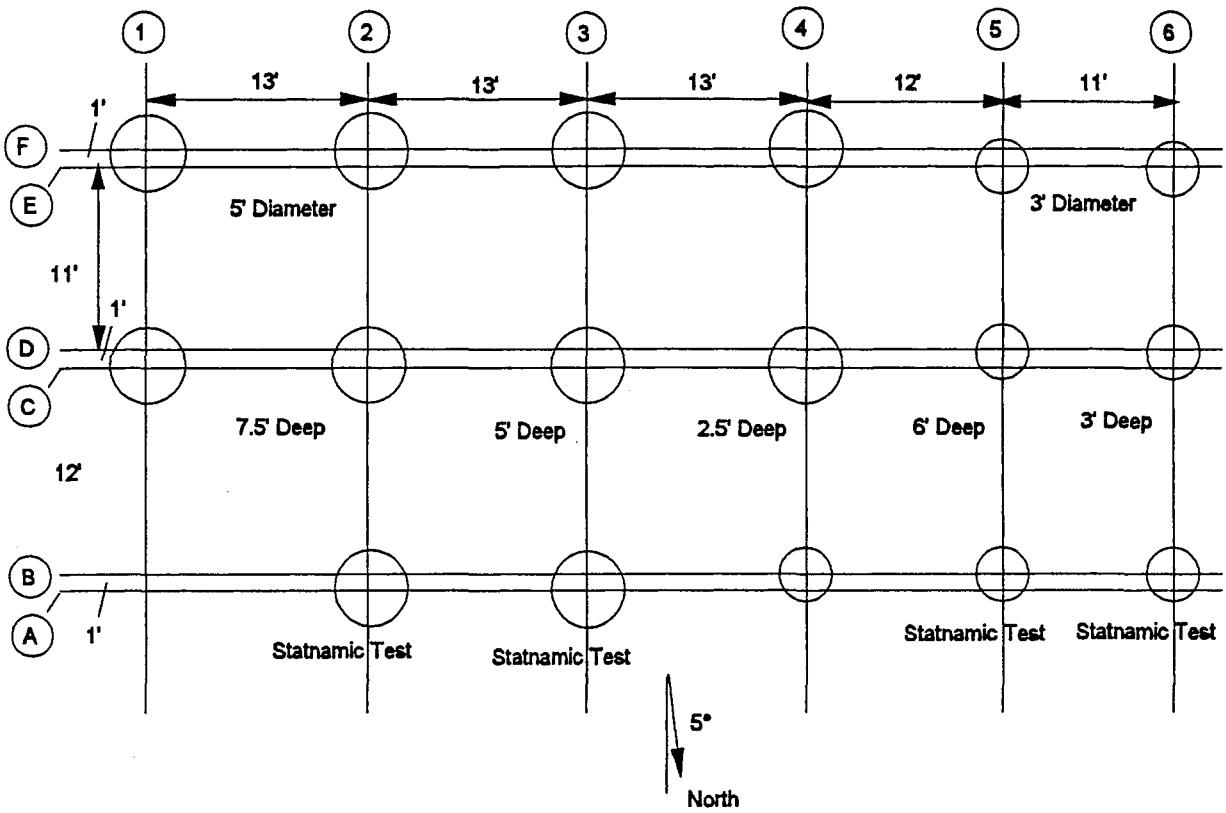

Figure 1 Spring Villa Test Site Layout

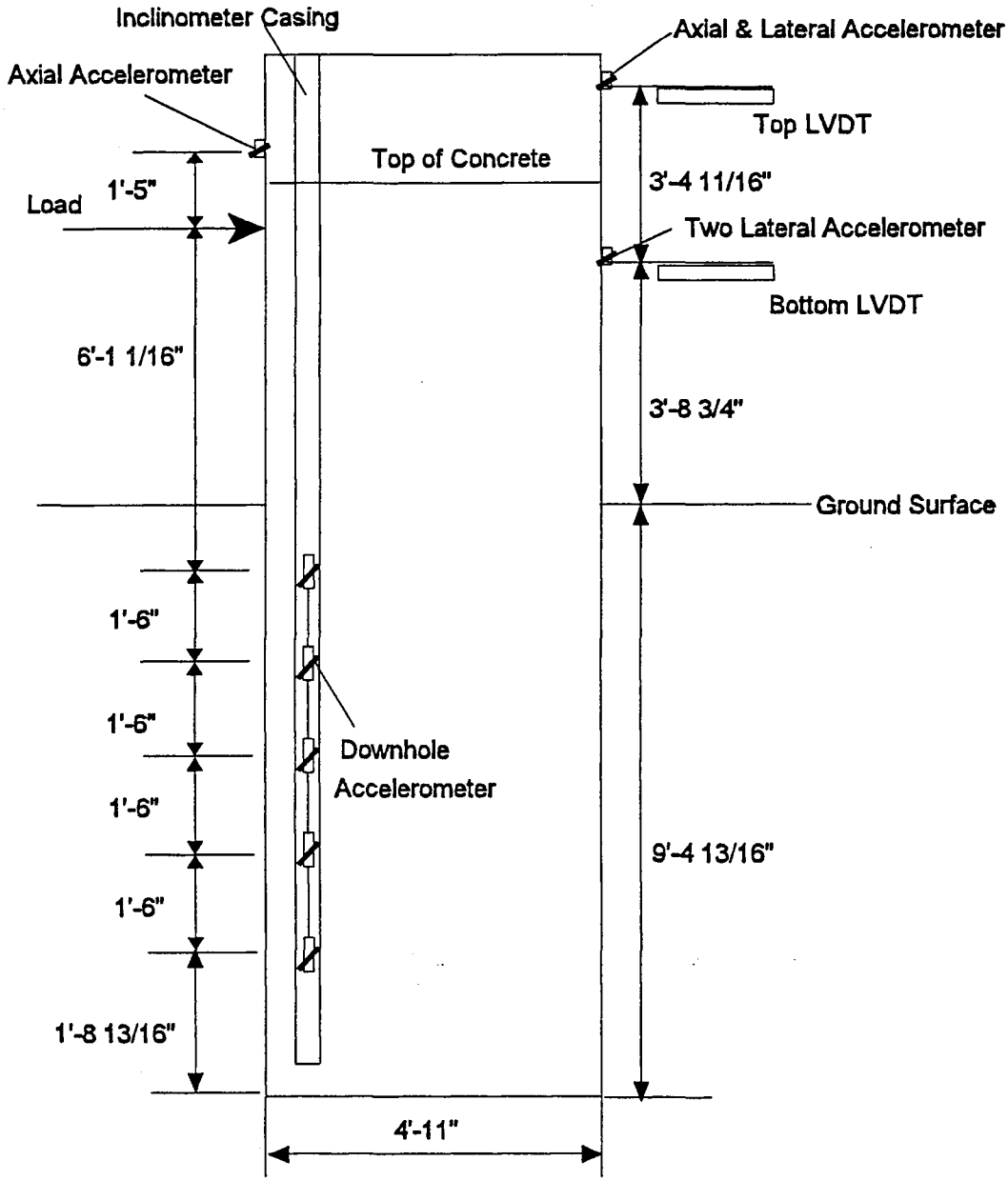

Figure 2 Test Setup, Shaft A2

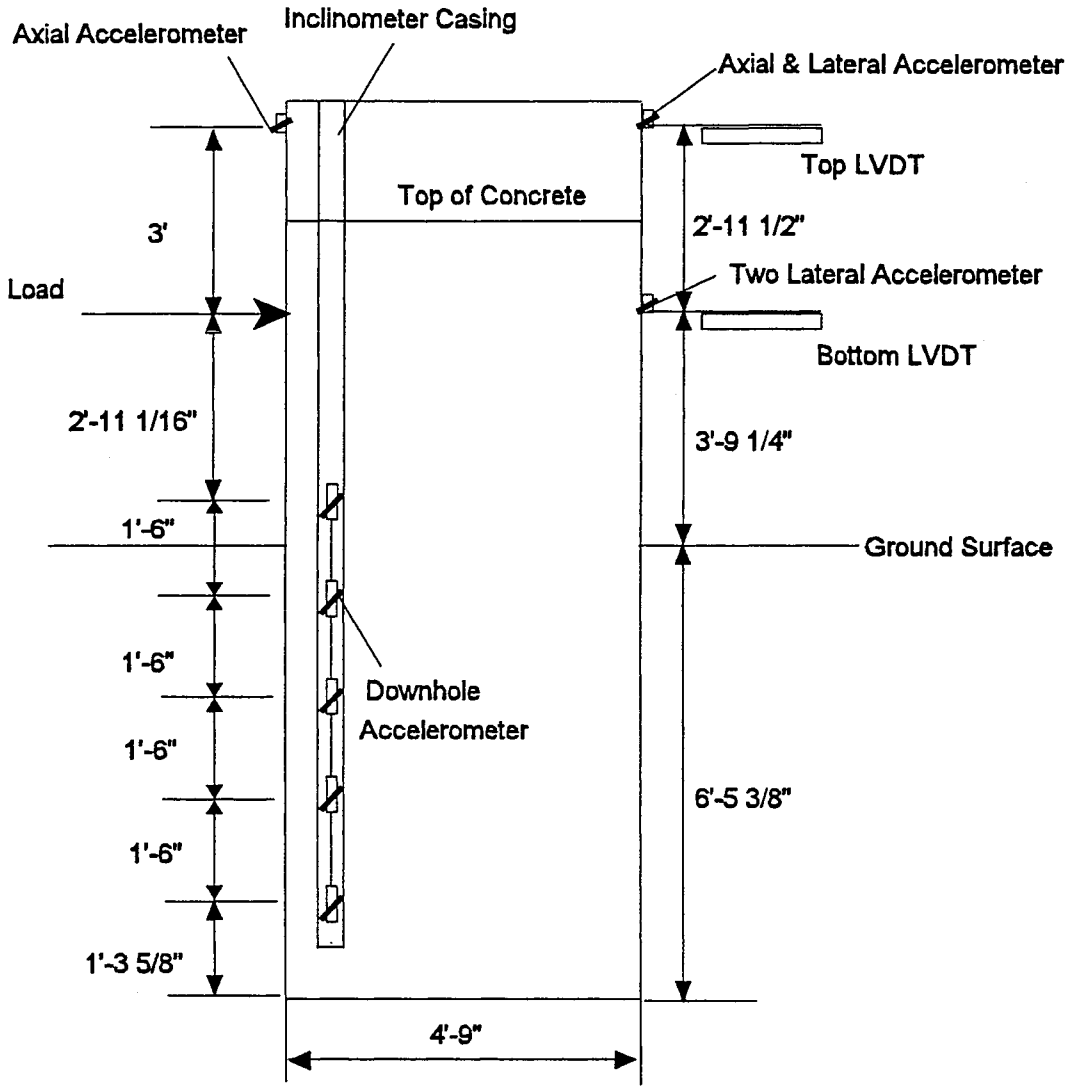

Figure 3 Test Setup, Shaft A3

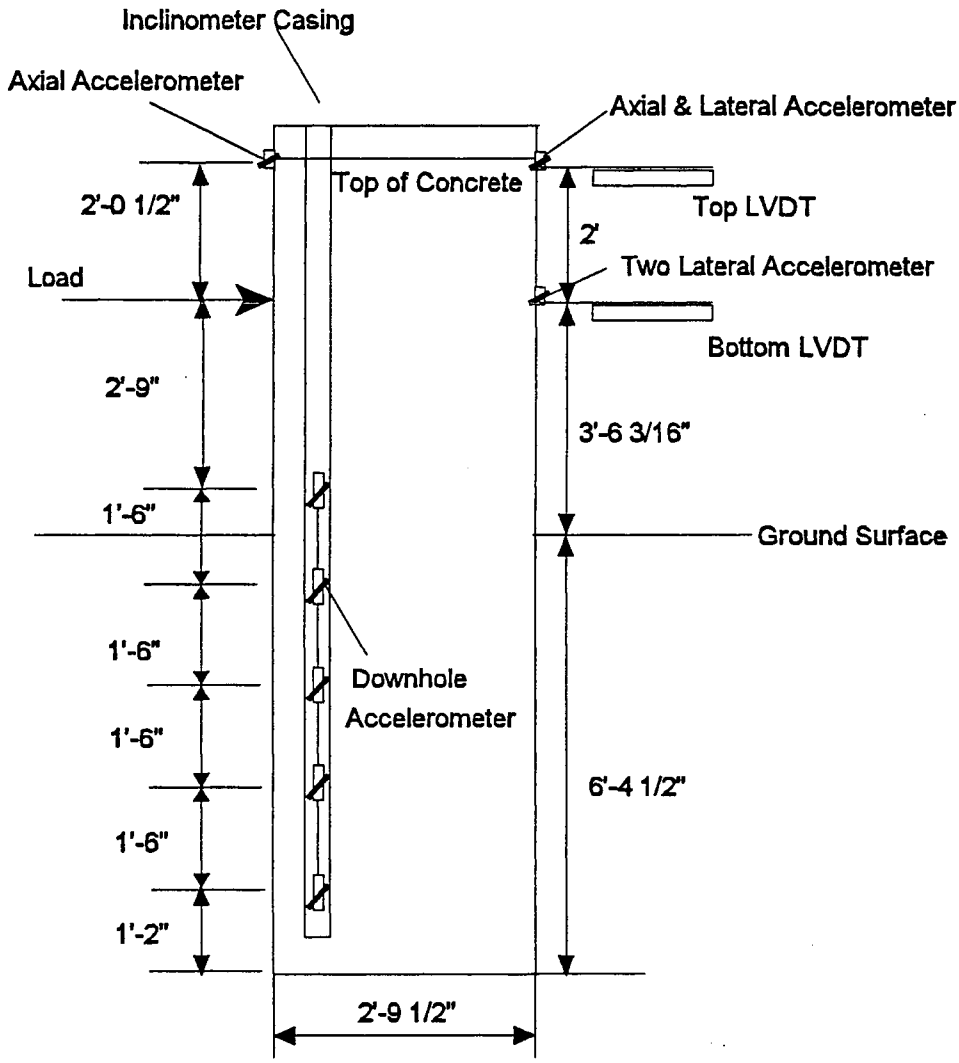

Figure 4, Test Setup, Shaft B5

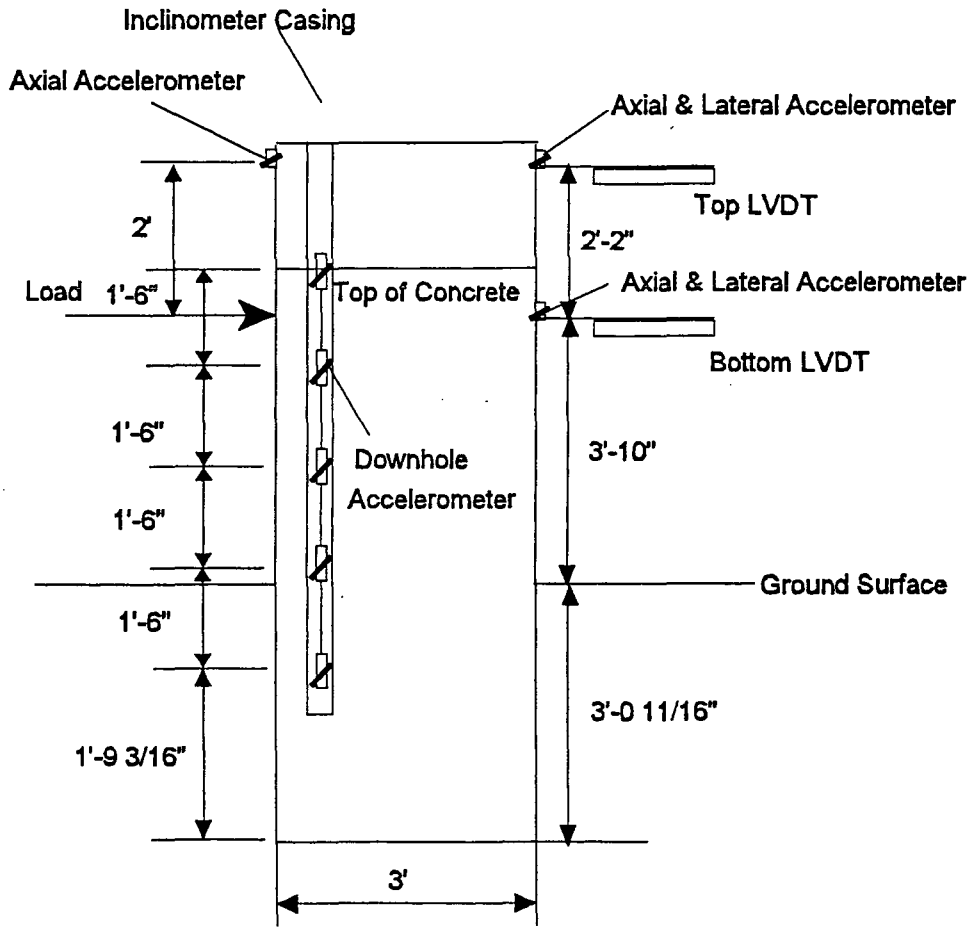

Figure 5 Test Setup, Shaft B6

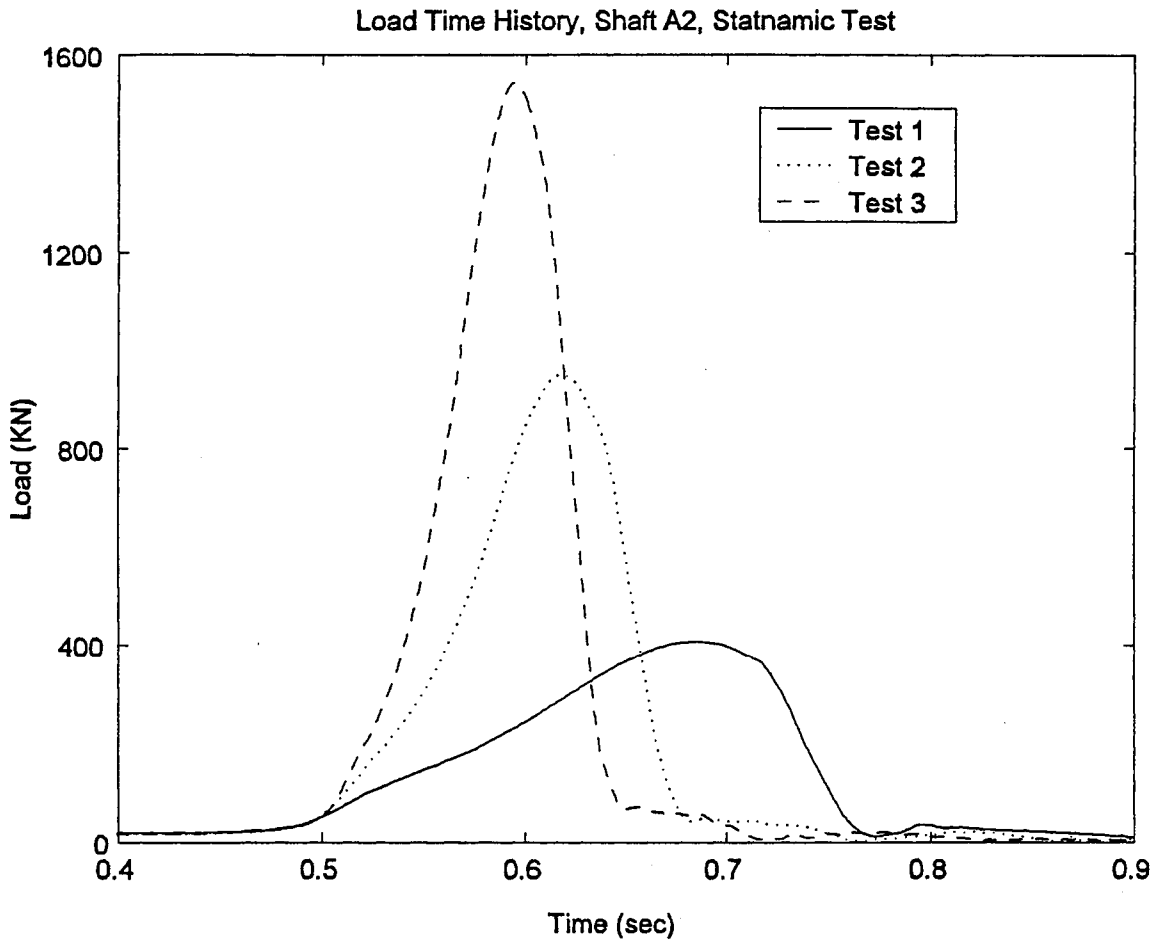

Figure 6 Load Time History, Shaft A2

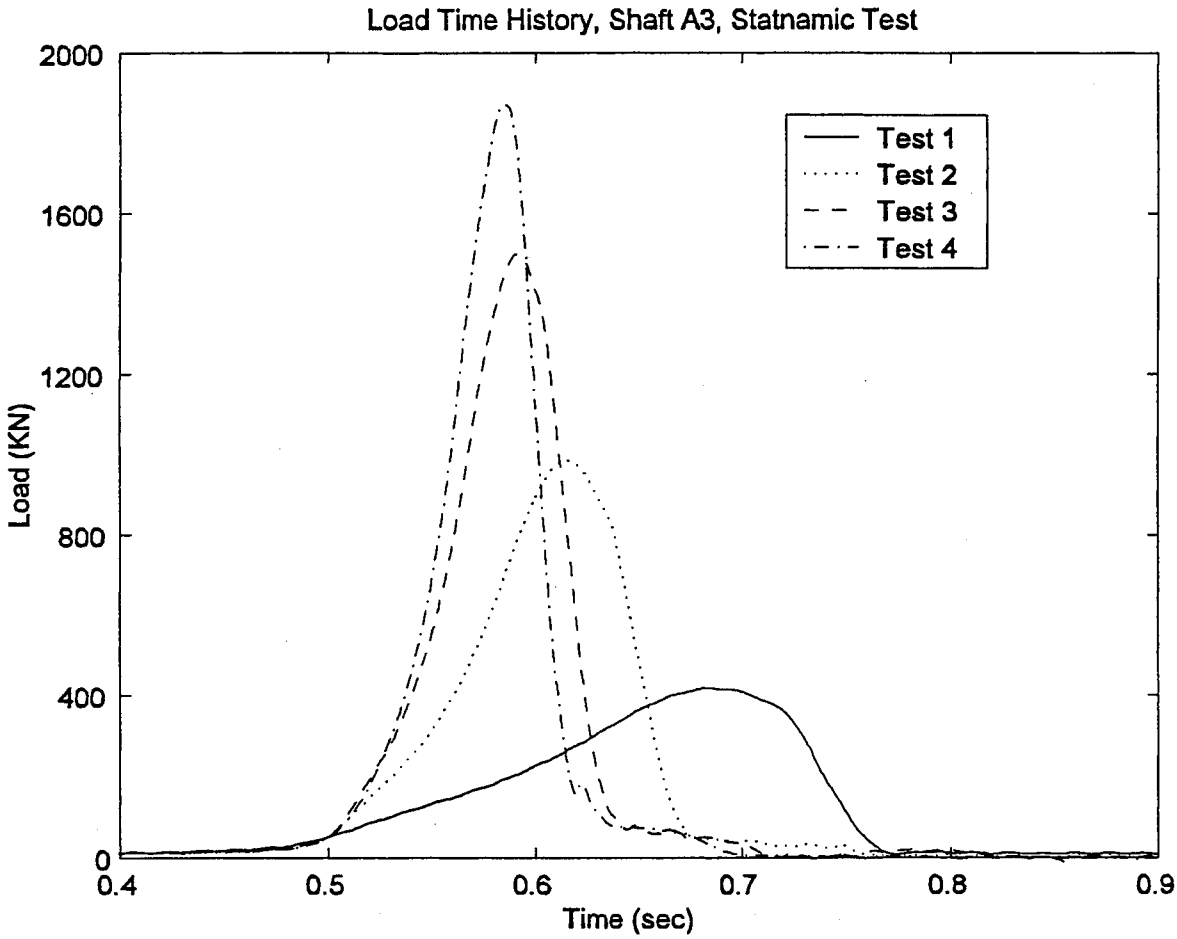

Figure 7 Load Time History, Shaft A3

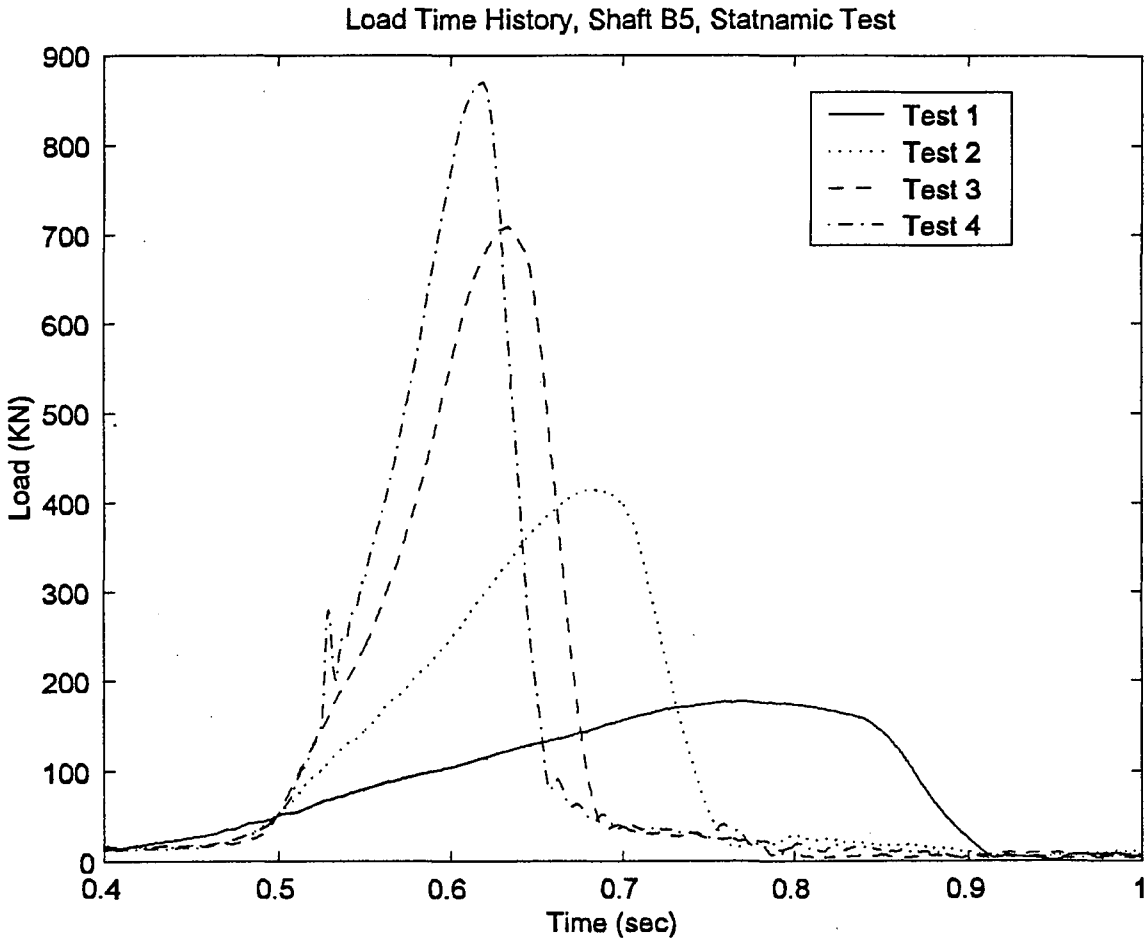

Figure 8 Load Time History, Shaft B5

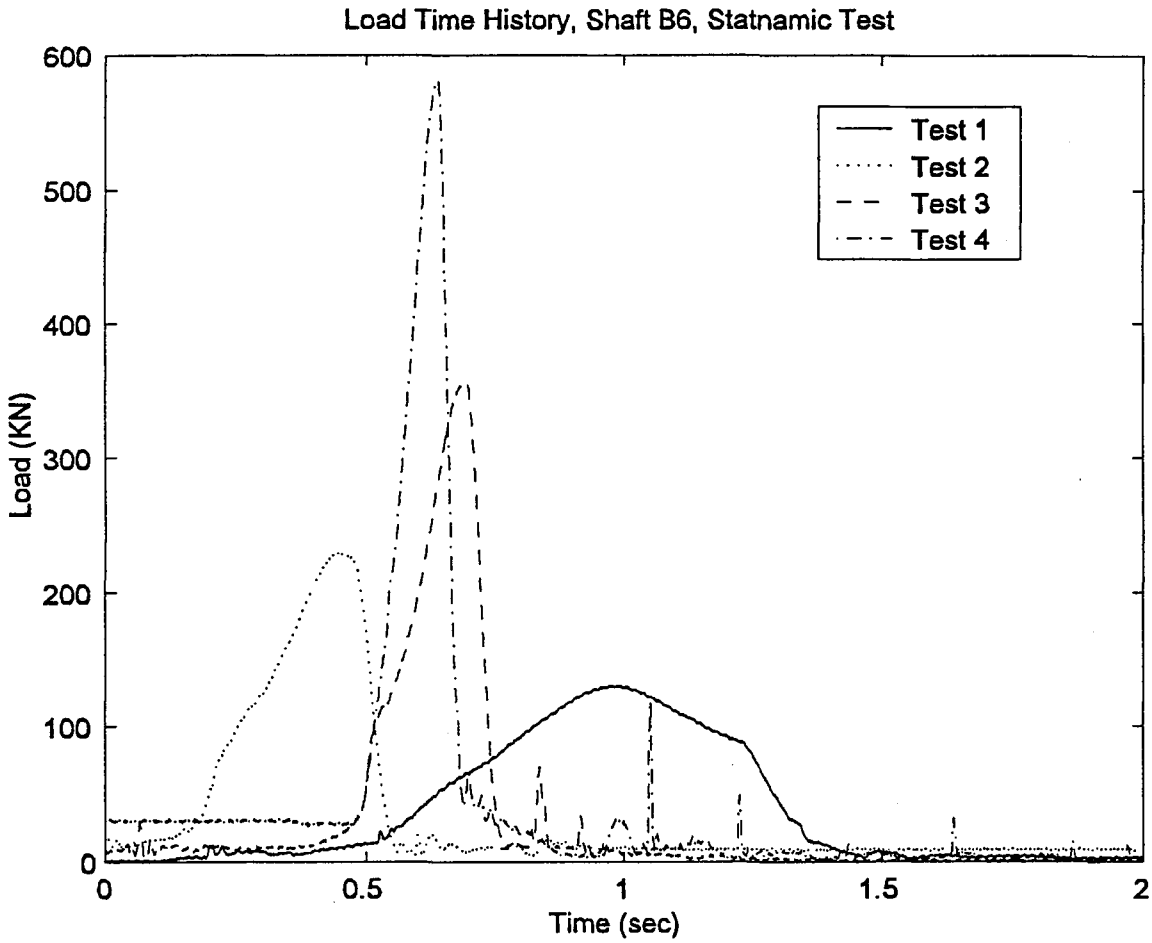

Figure 9 Load Time History, Shaft B6

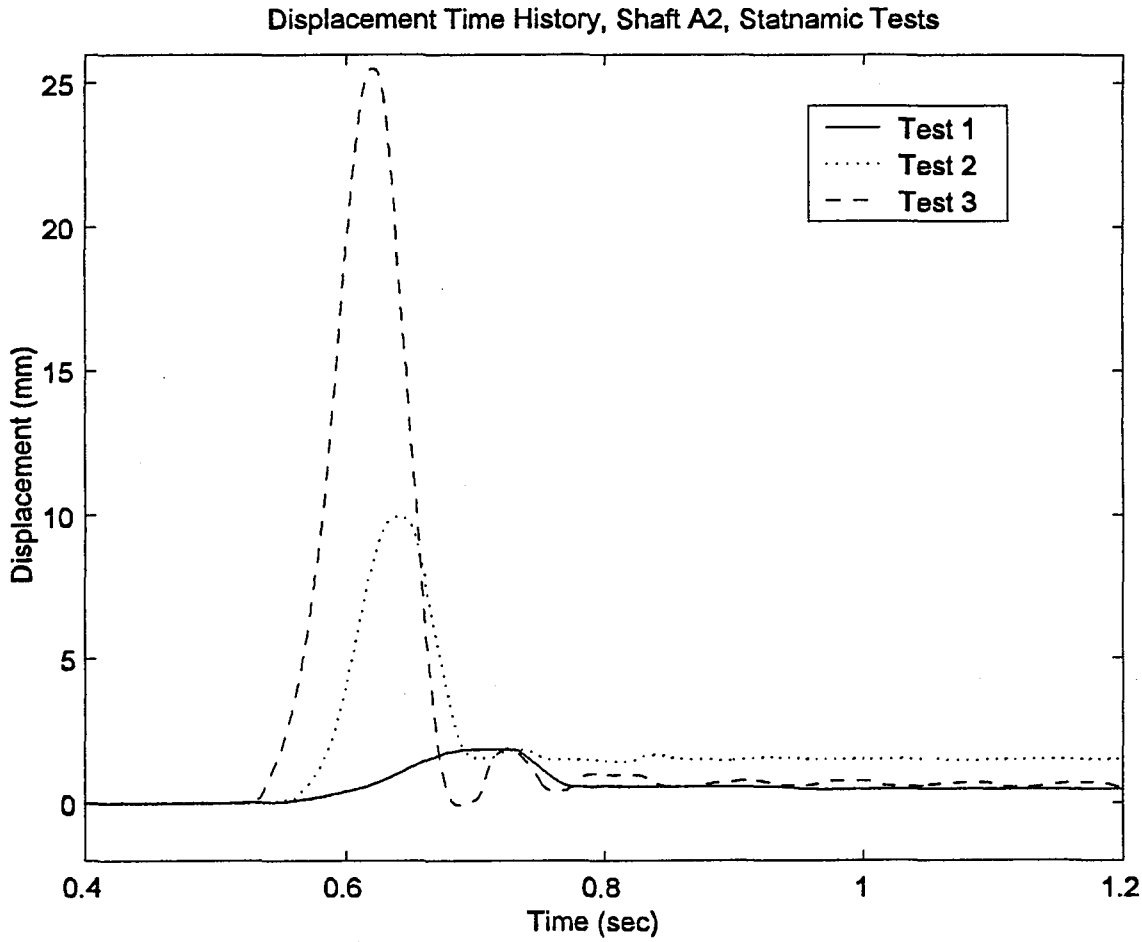

Figure 10 Displacement Time History, Shaft A2

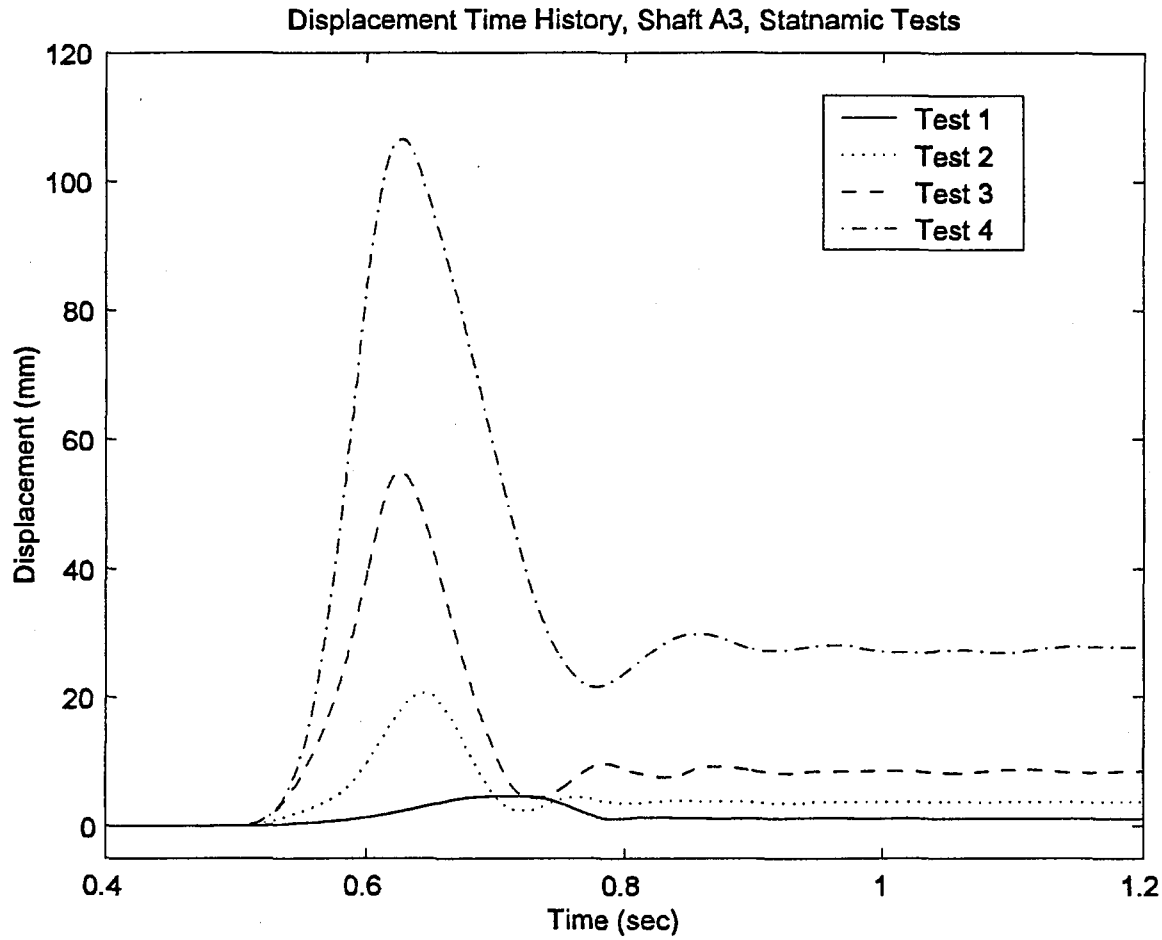

Figure 11 Displacement Time History, Shaft A3

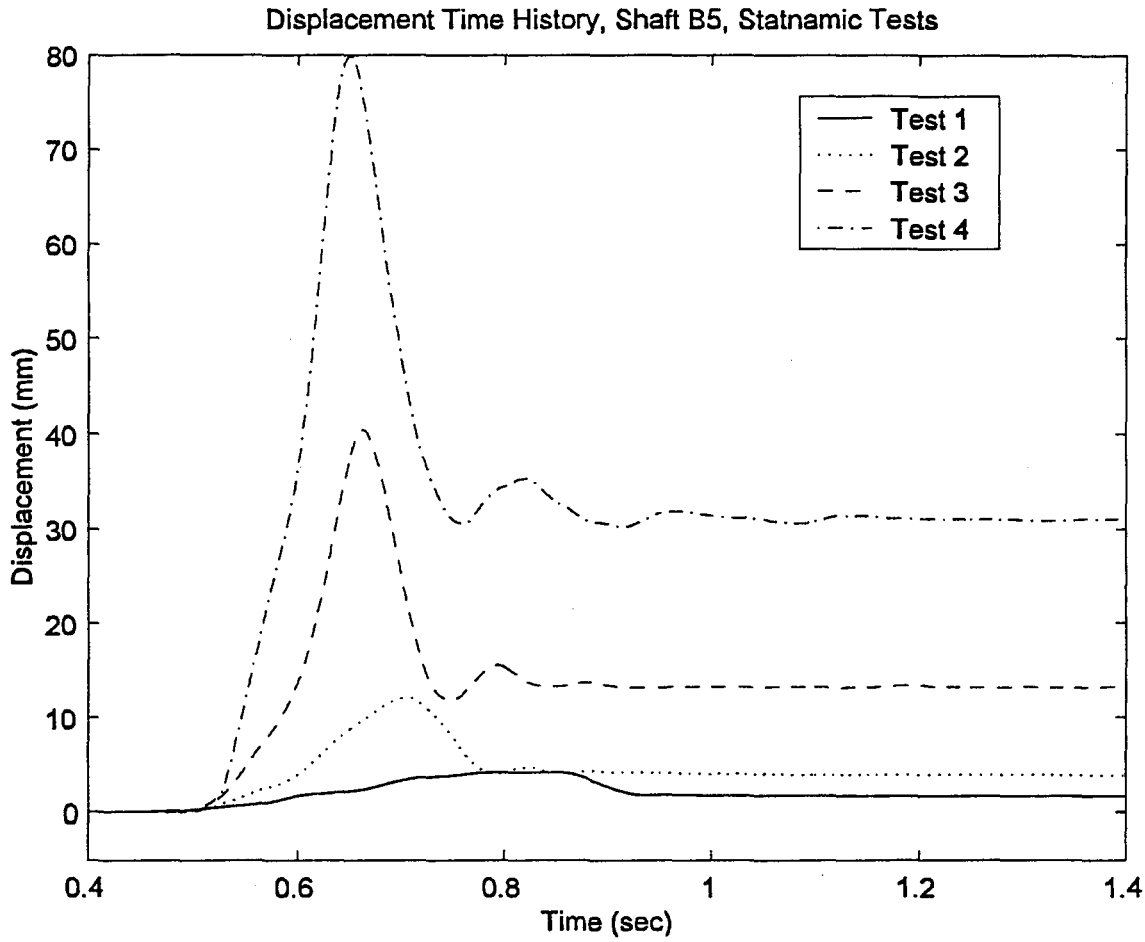

Figure 12 Displacement Time History, Shaft B5

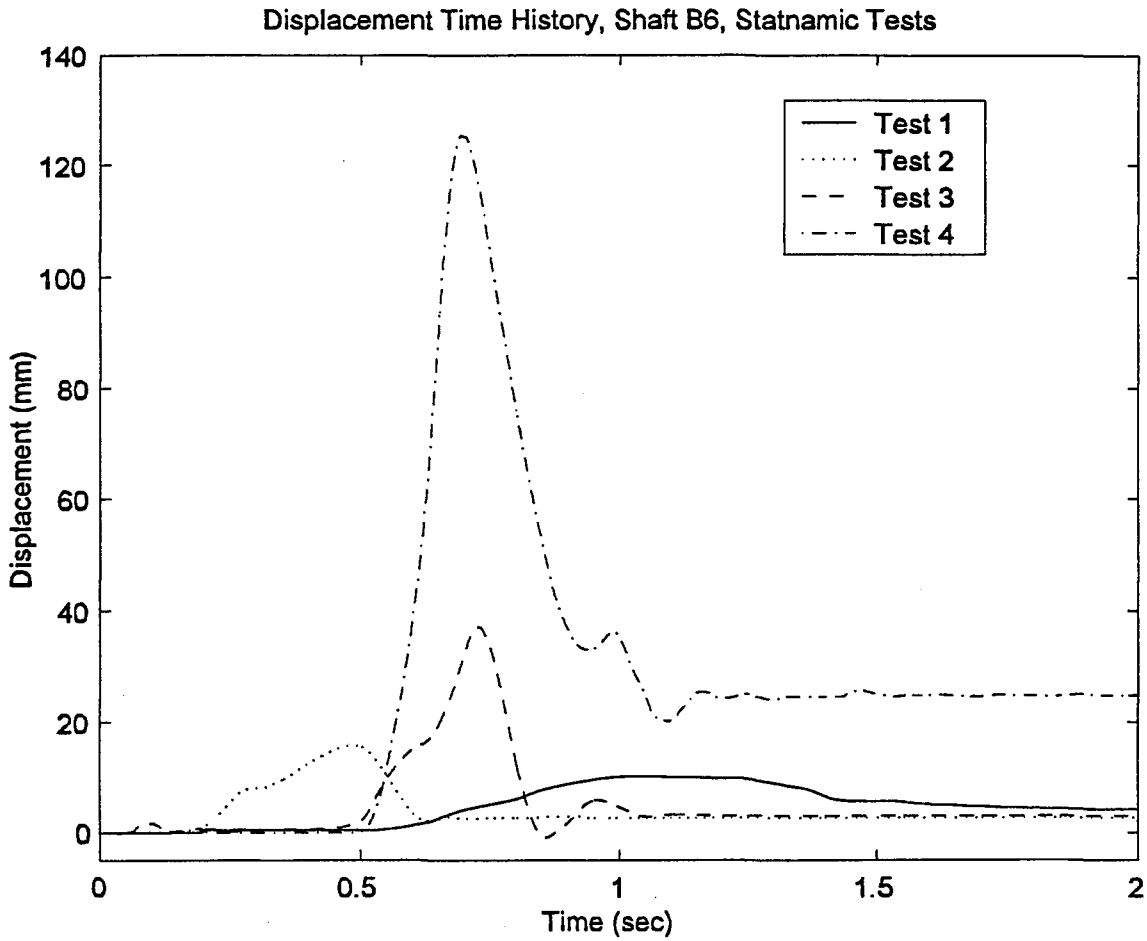

Figure 13 Displacement Time History, Shaft B6

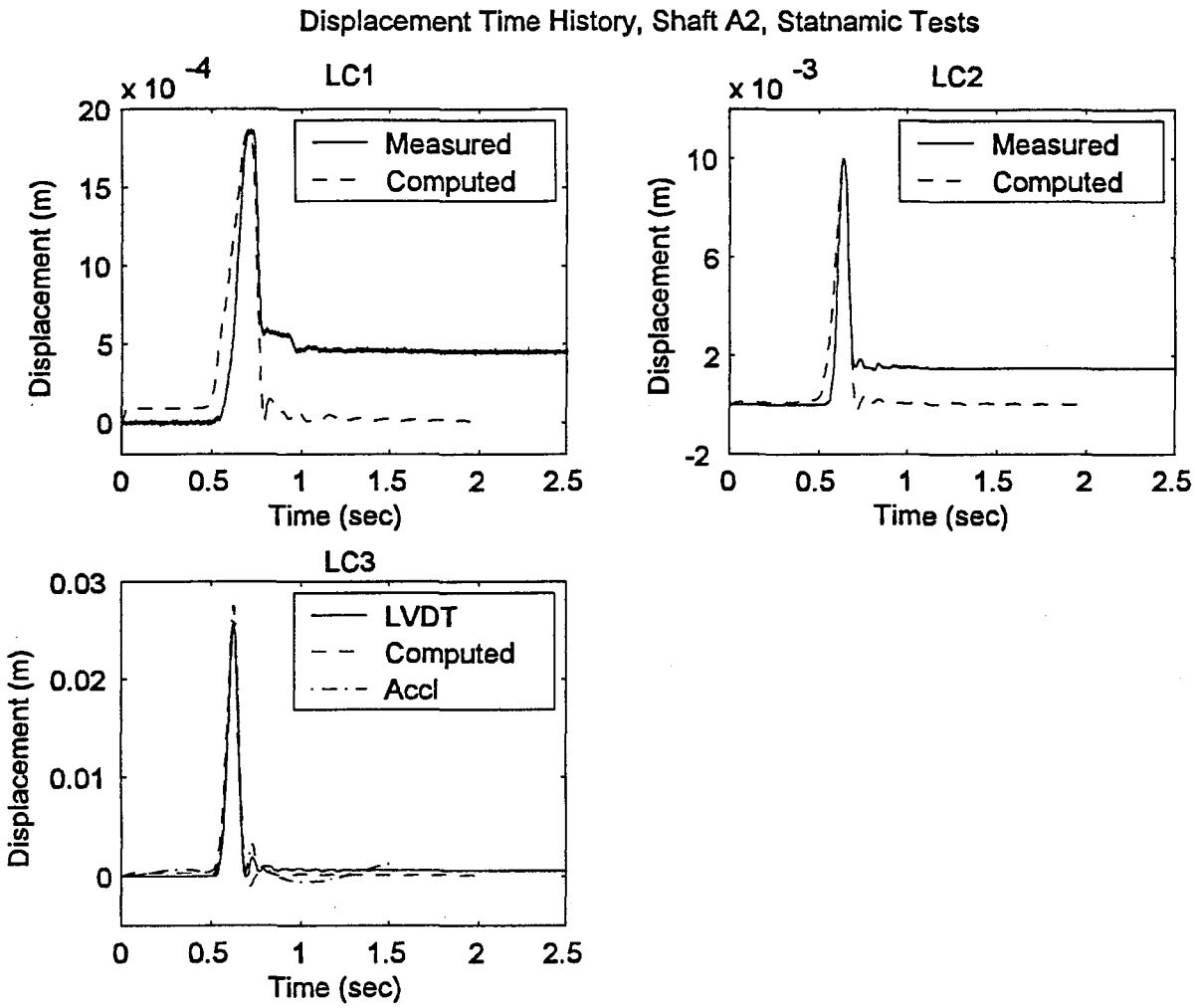

Figure 14 Measured and Computed Displacement Response, Shaft A2

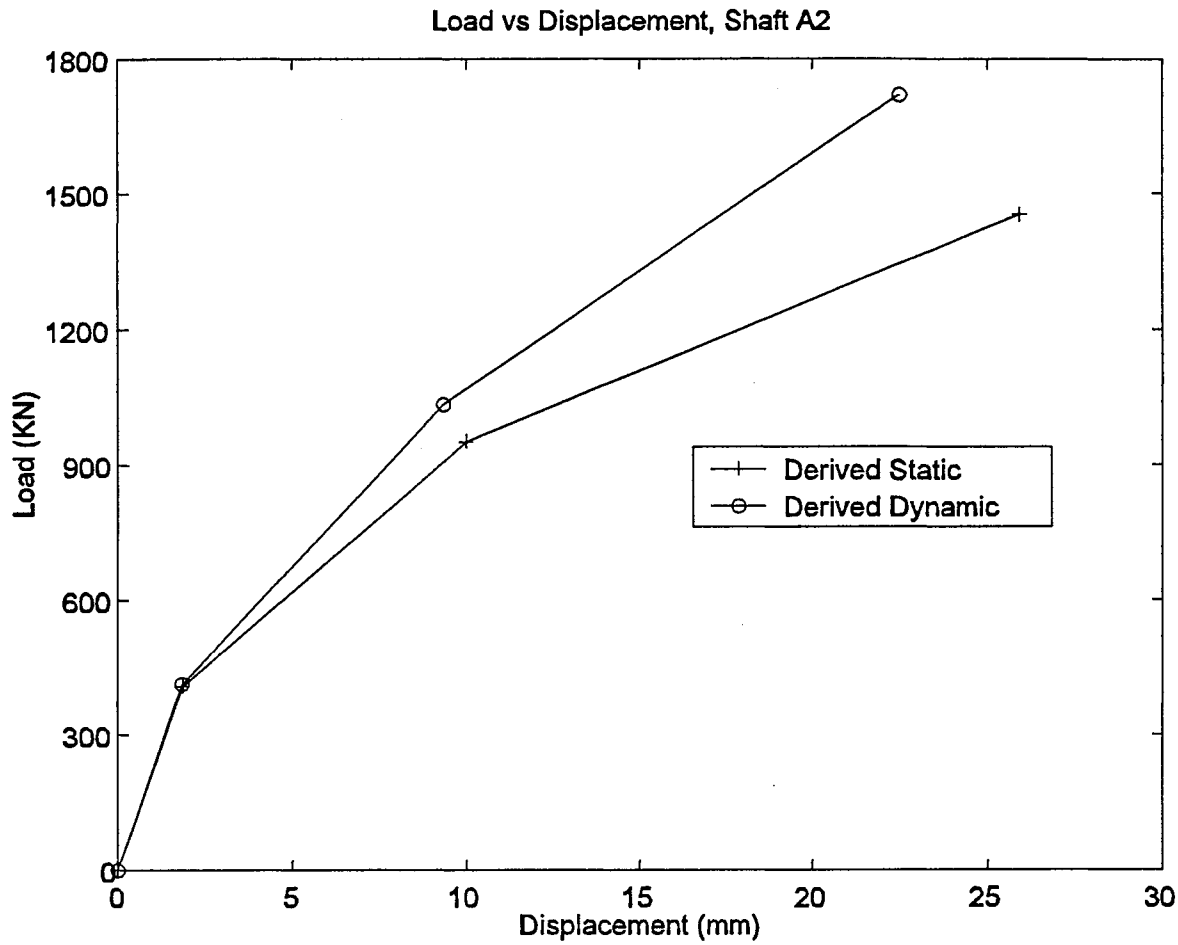

Figure 15 Derived Load Displacement Response, Shaft A2

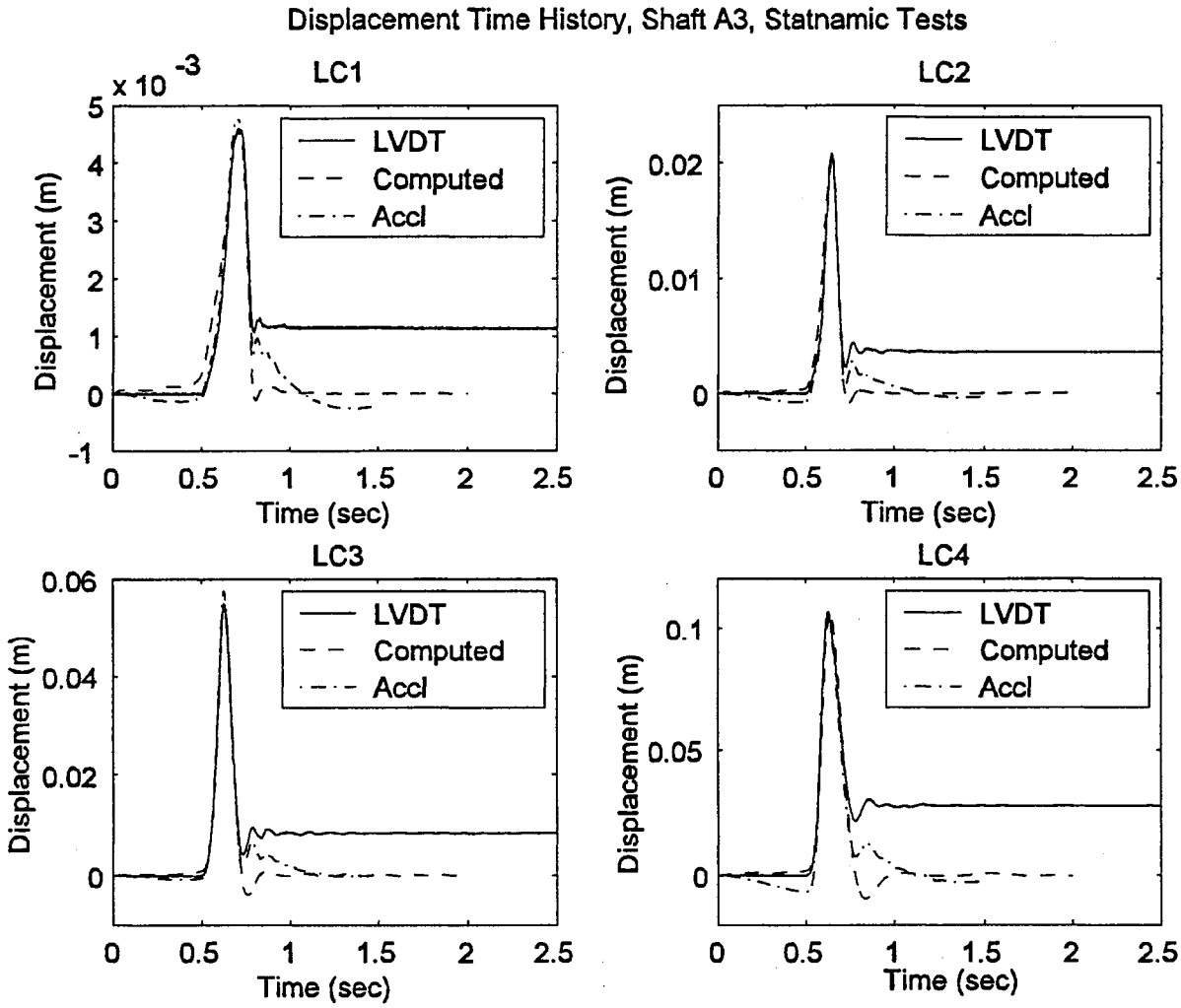

Figure 16 Measured and Computed Displacement Response, Shaft A3

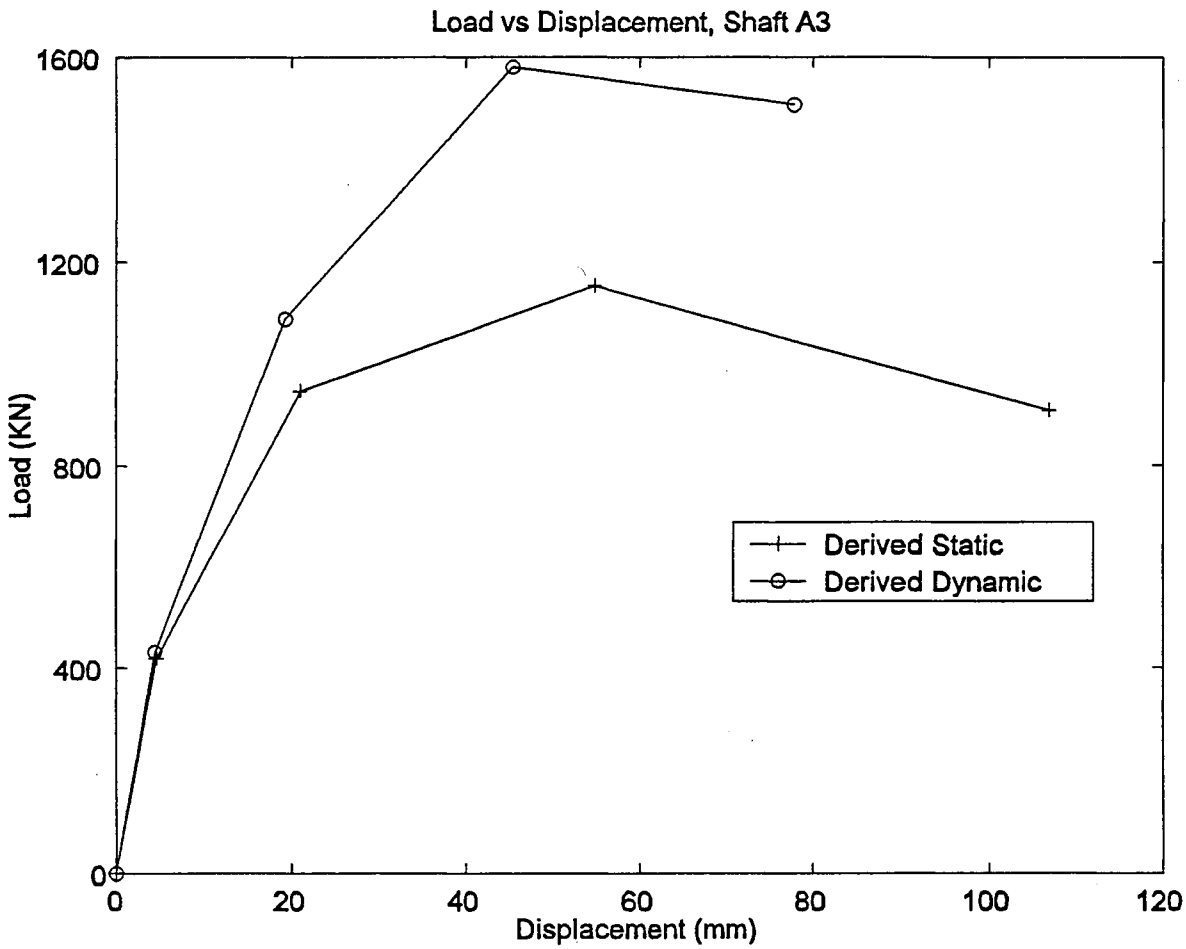

Figure 17 Derived Load Displacement Response, Shaft A3

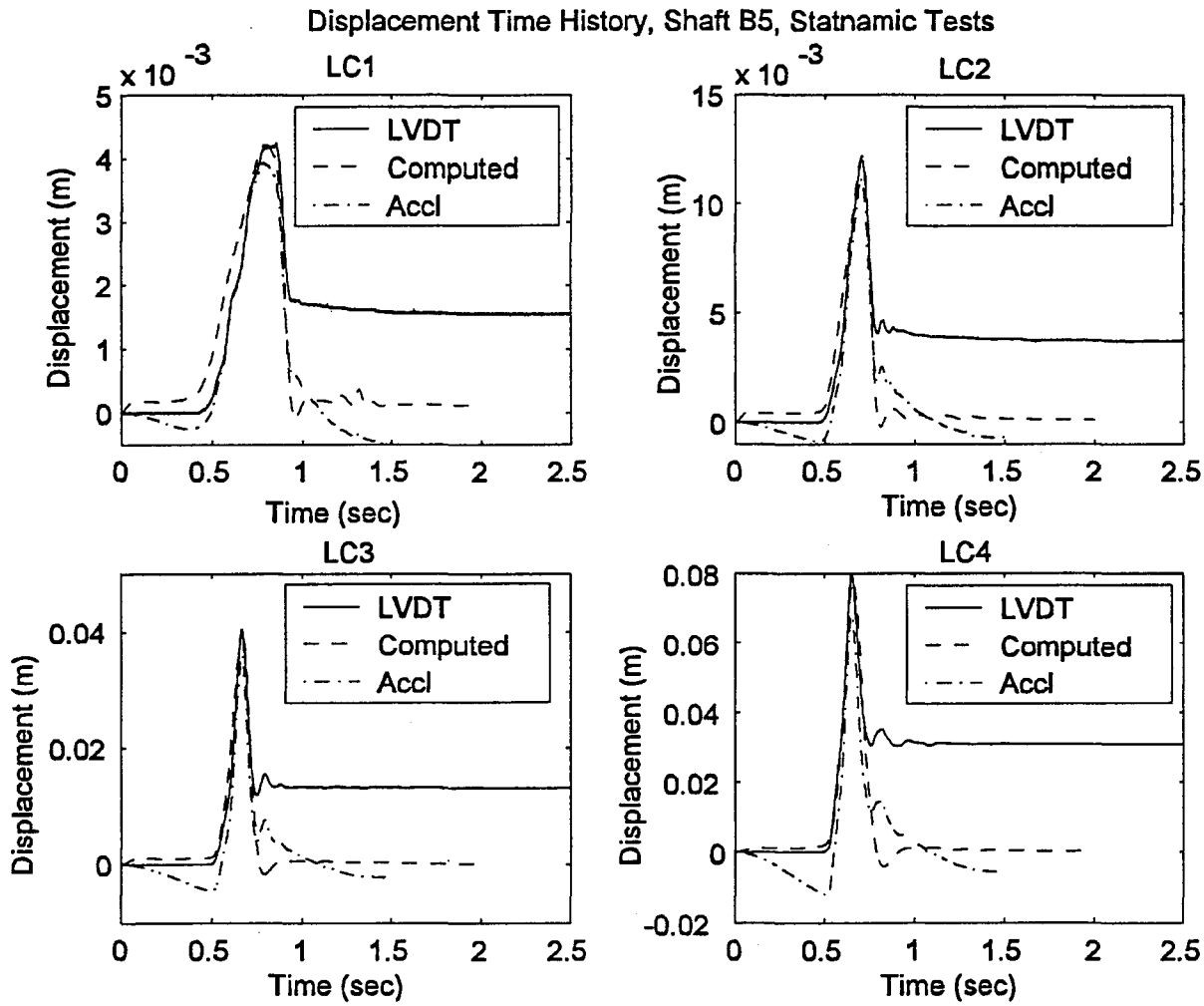

Figure 18 Measured and Computed Displacement Response, Shaft B5

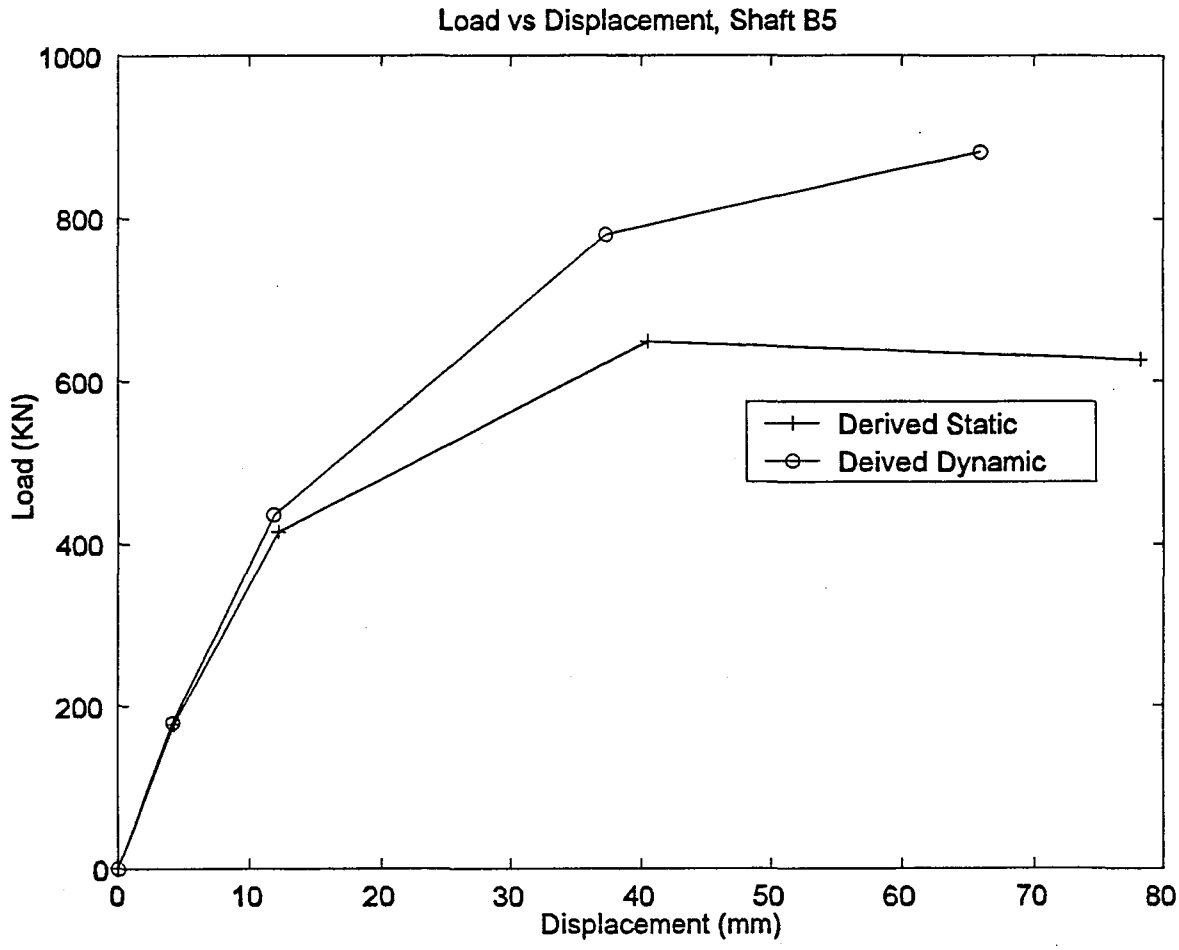

Figure 19 Derived Load Displacement Response, Shaft B5

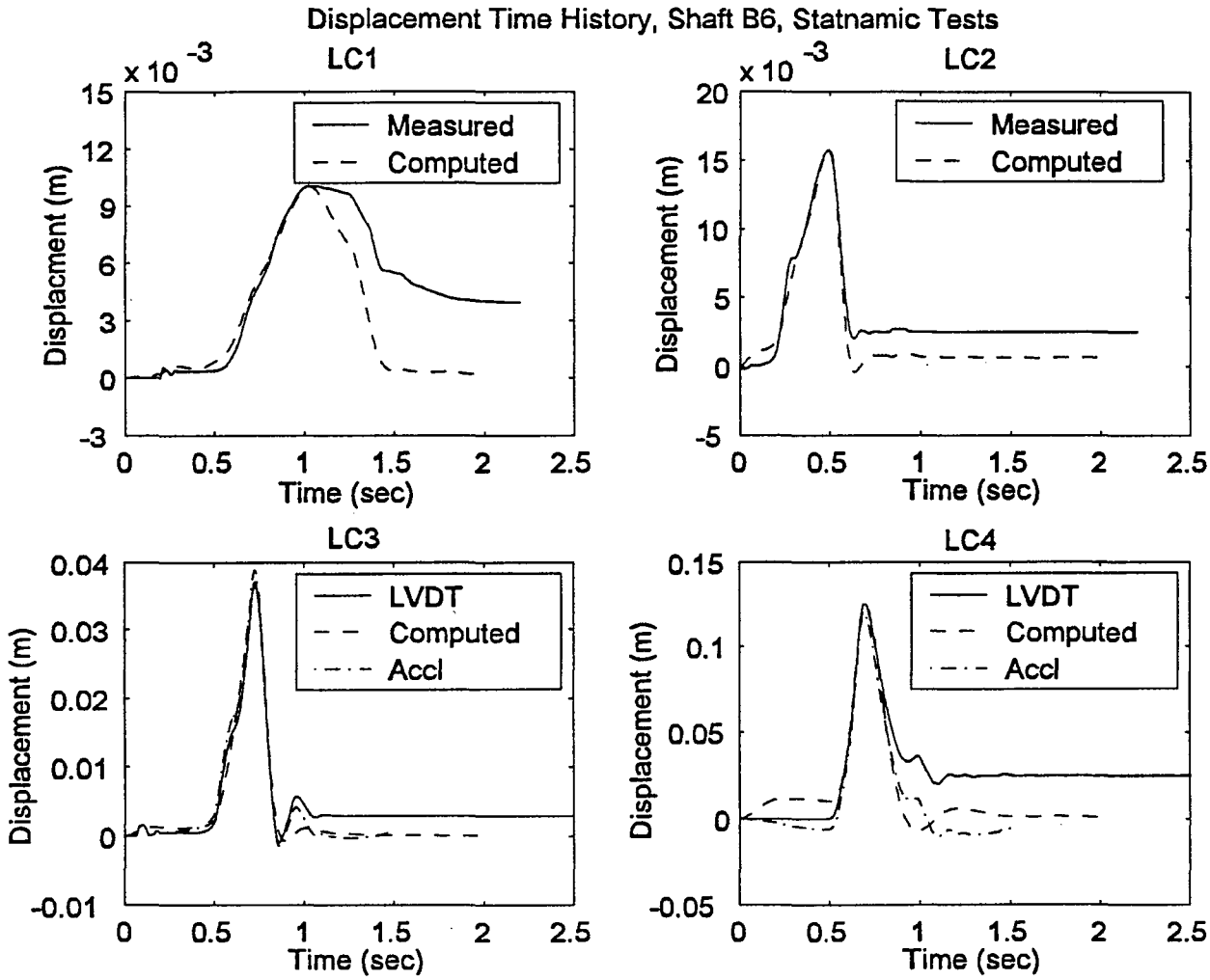

Figure 20 Measured and Computed Displacement Response, Shaft B6

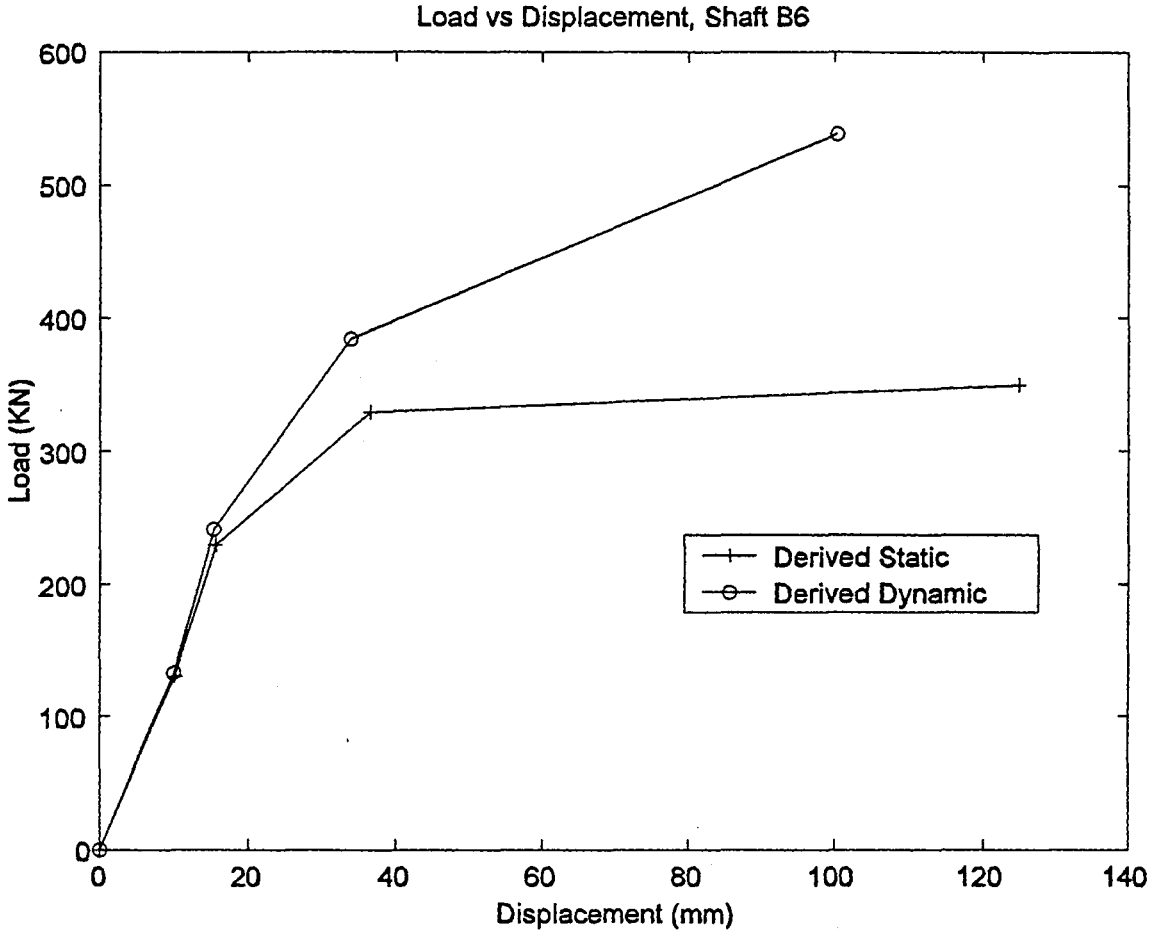

Figure 21 Derived Load Displacement Response, Shaft B6

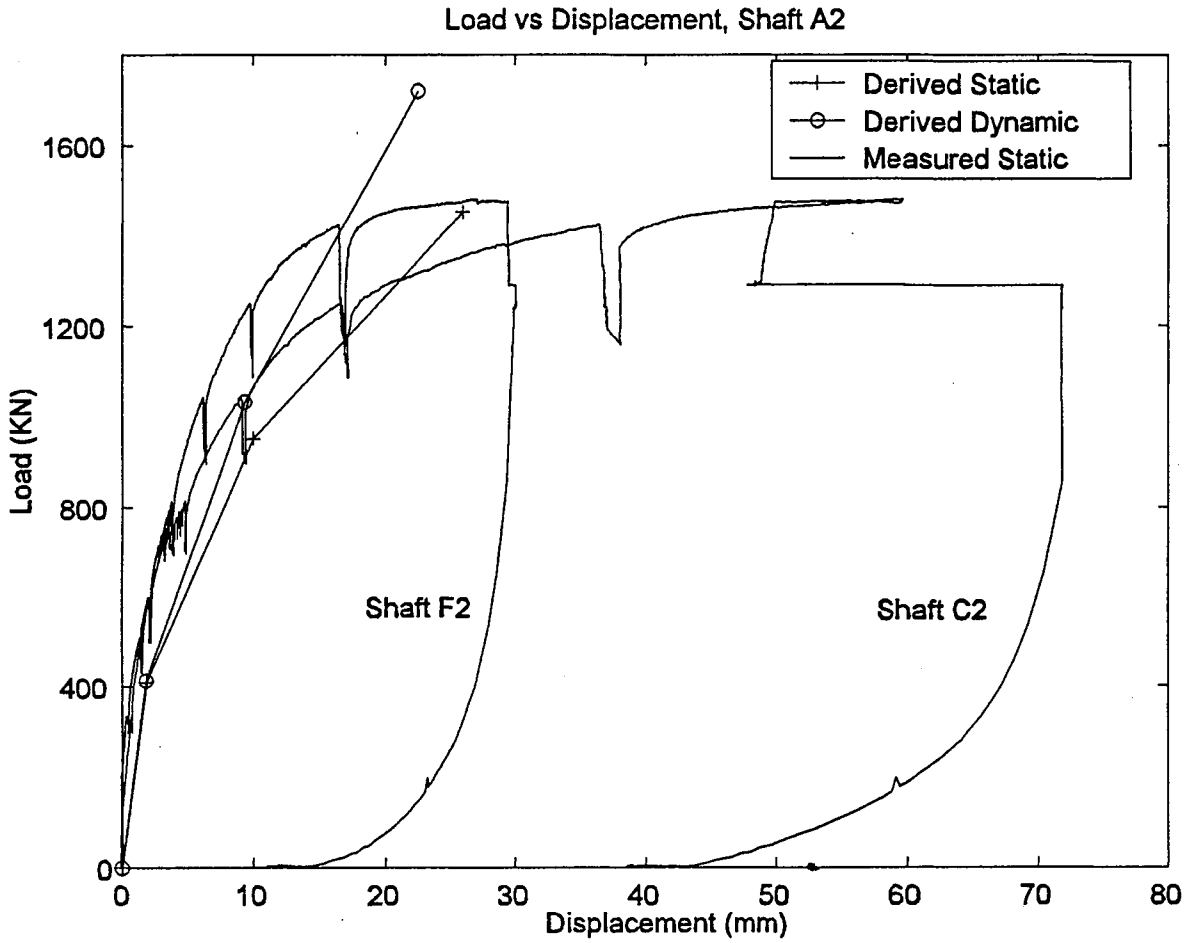

Figure 22 Comparison of Statnamic and Static Test, Shaft A2

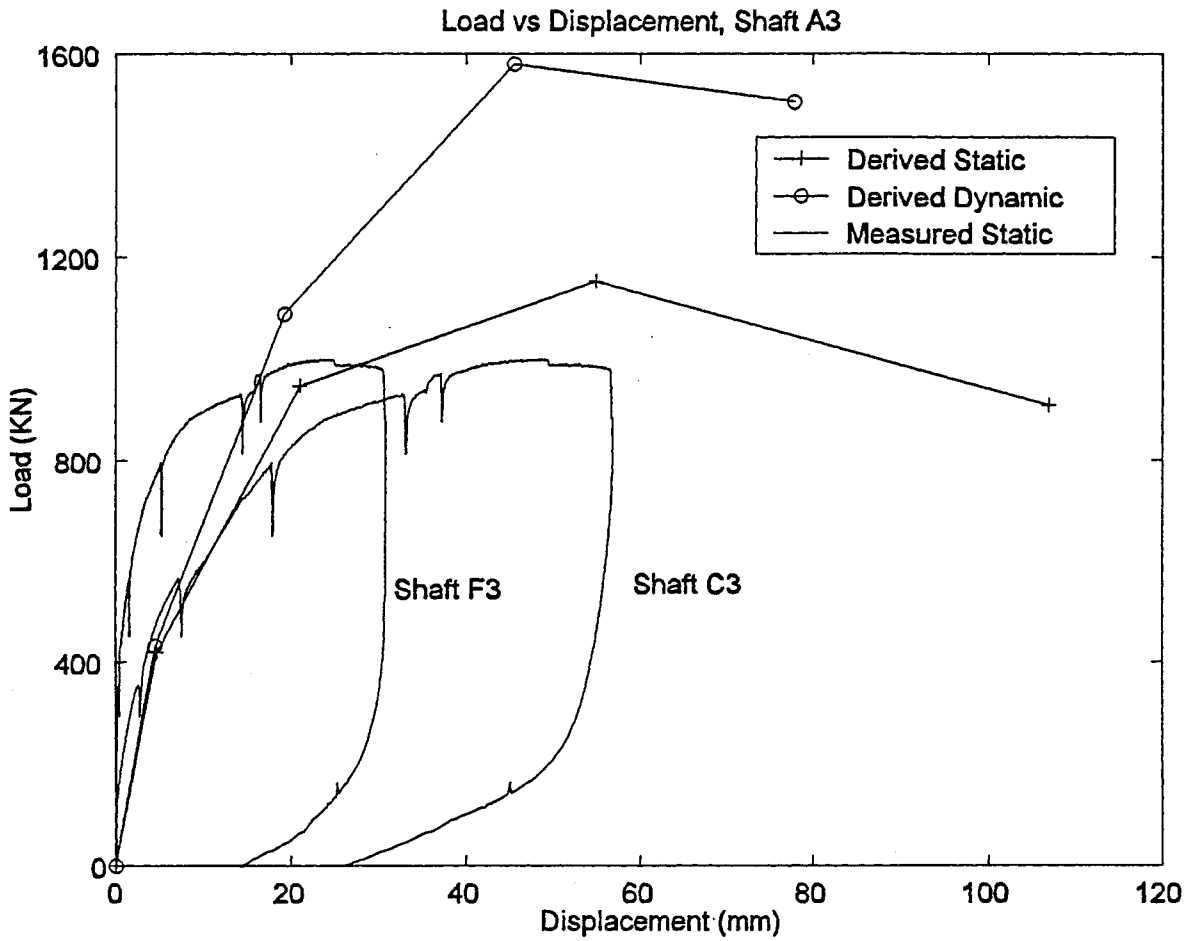

Figure 23 Comparison of Statnamic and Static Test, Shaft A3

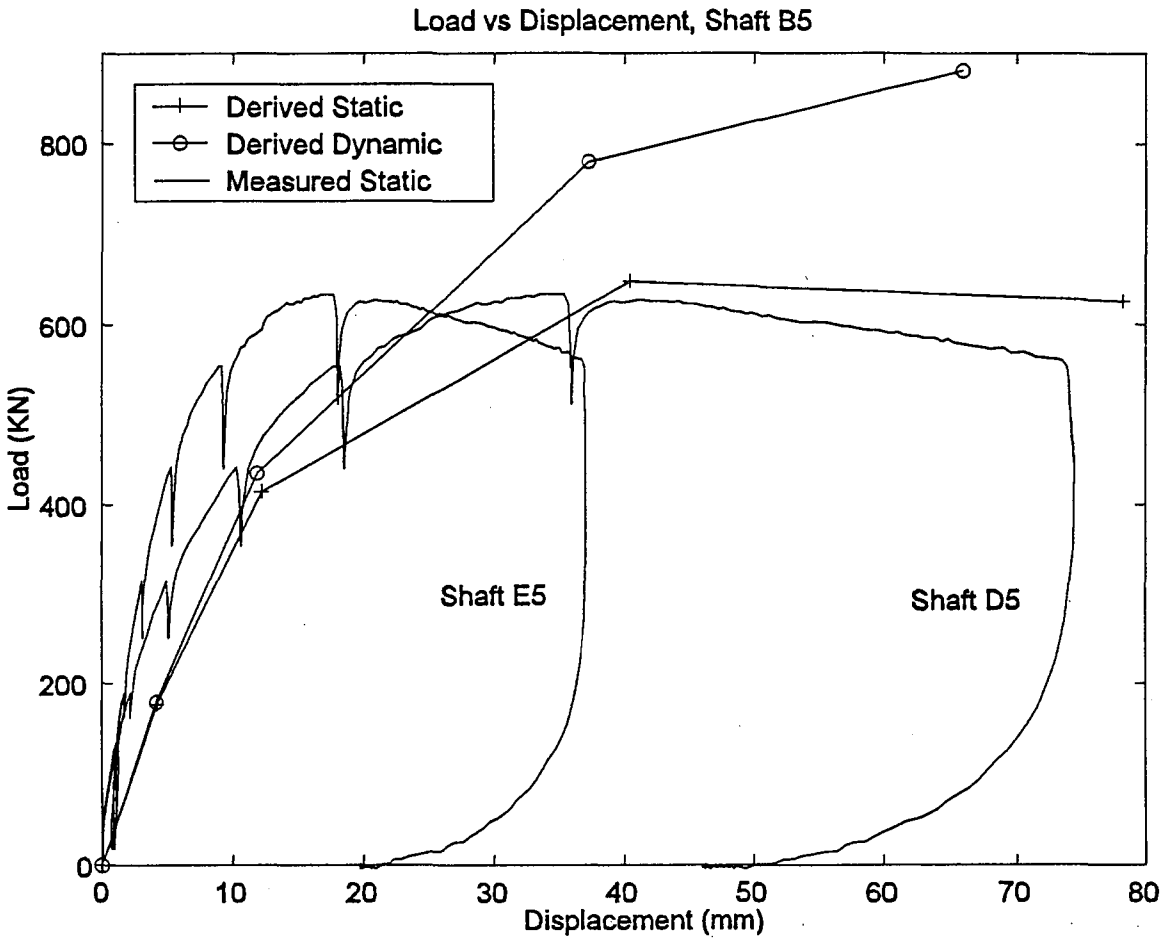

Figure 24 Comparison of Statnamic and Static Test, Shaft B5

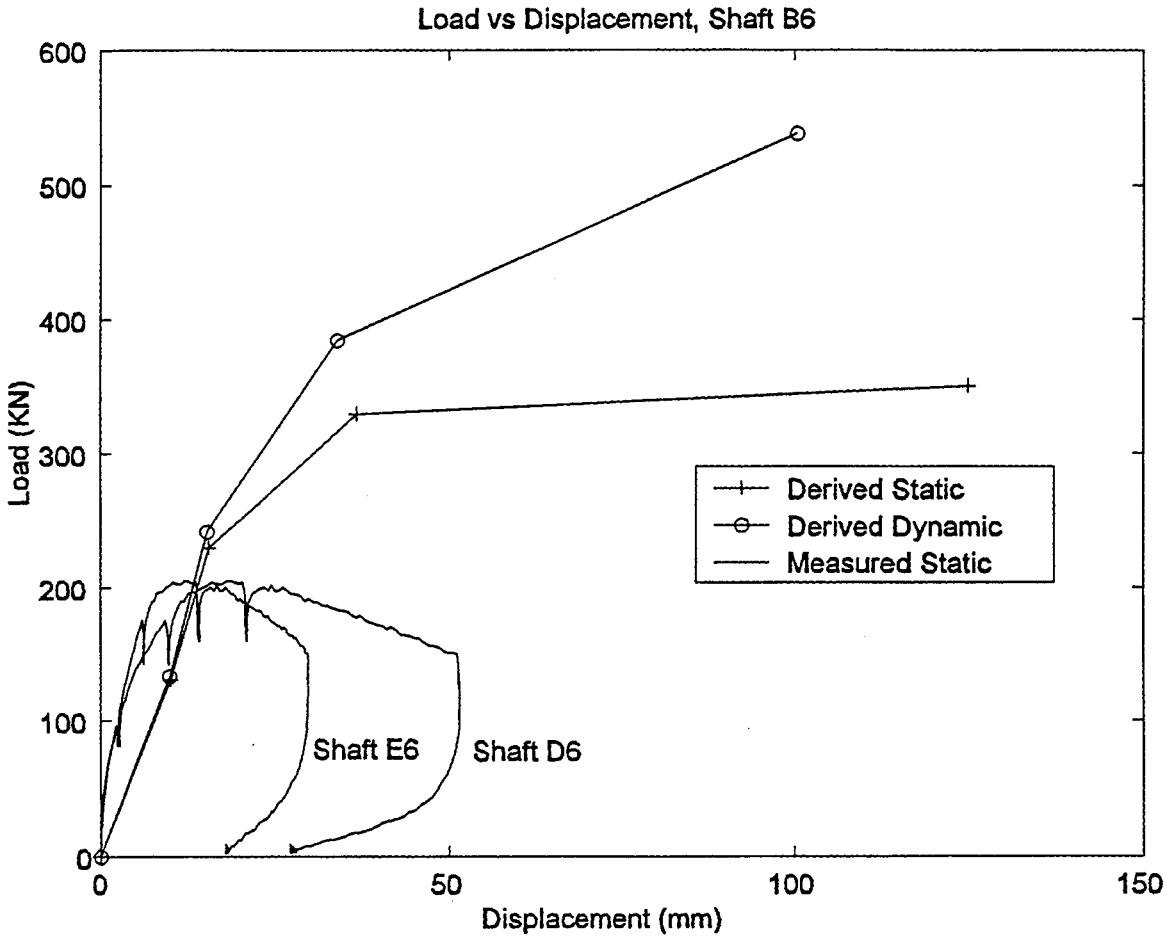

Figure 25 Comparison of Statnamic and Static Test, Shaft B6

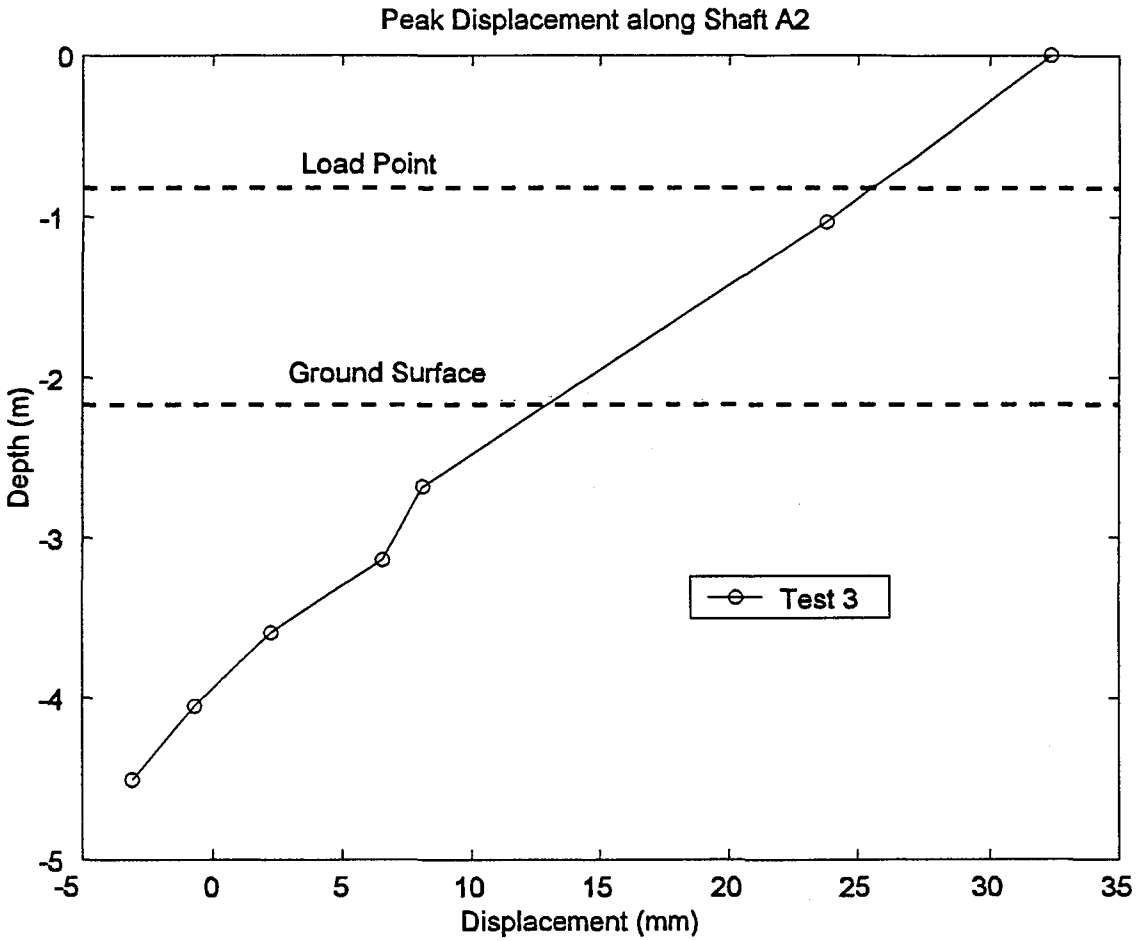

Figure 26 Displacement Profile along Shaft A2

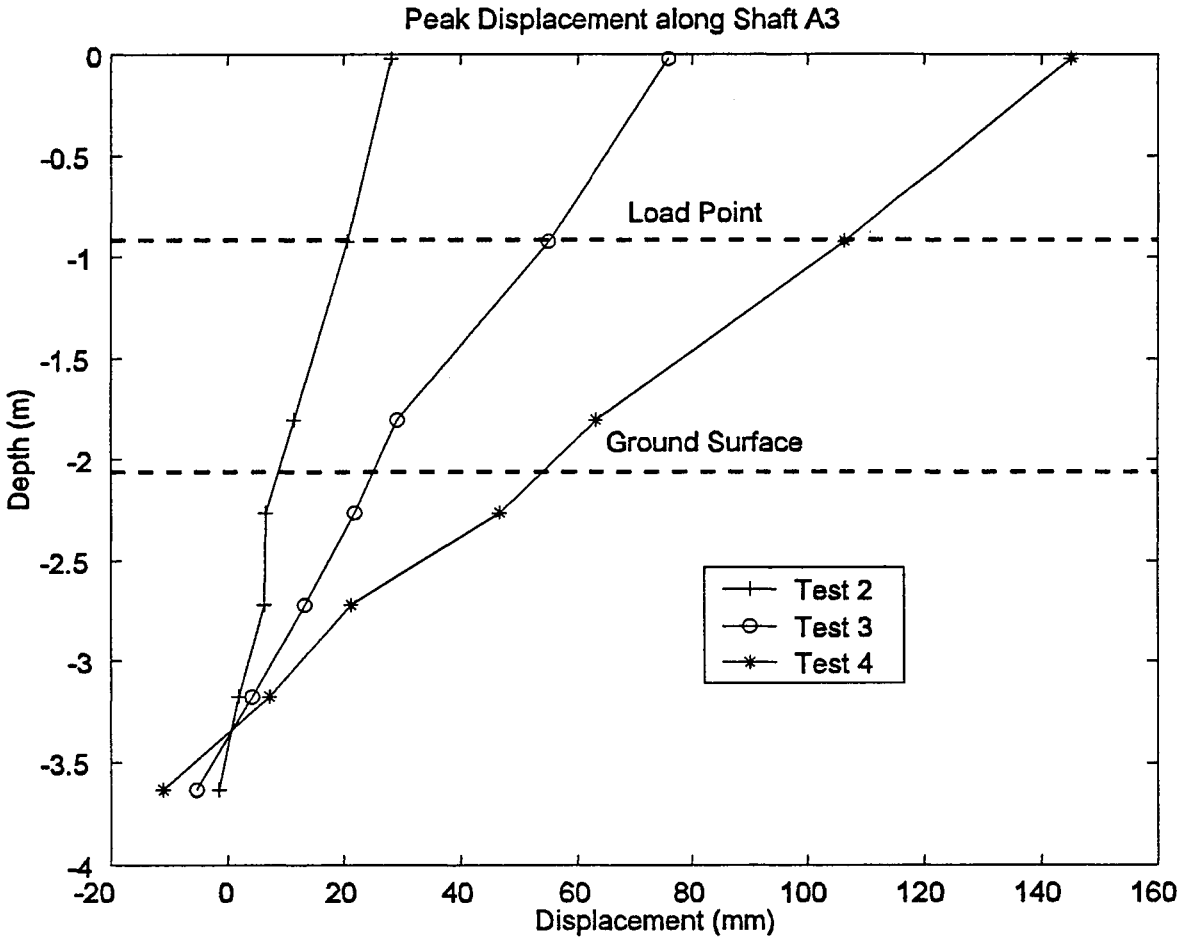

Figure 27 Displacement Profile along Shaft A3

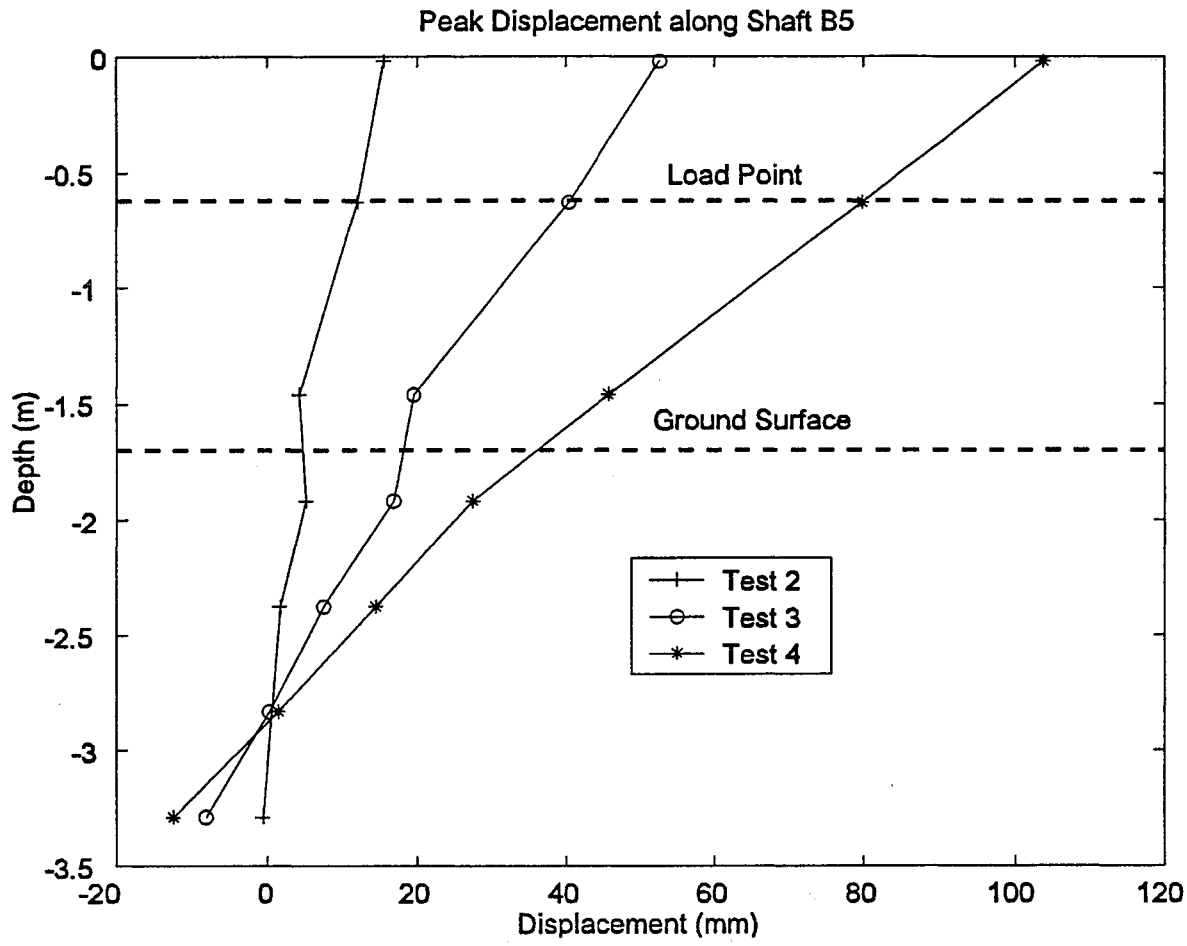

Figure 28 Displacement Profile along Shaft B5

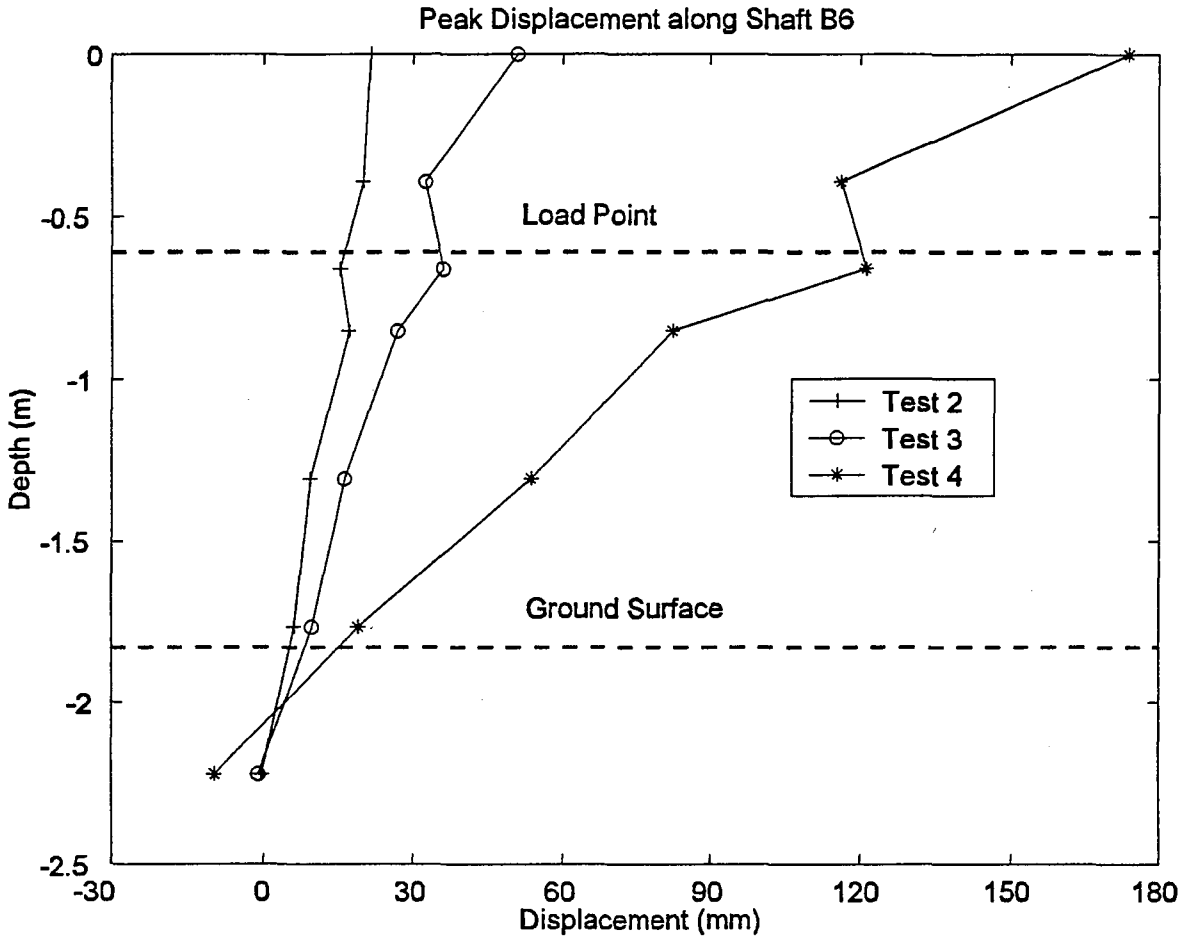

Figure 29 Displacement Profile along Shaft B6